NUSTAR Annual Meeting 2014
3-7 March 2014 GSI

Recent Developments in Theory of Nuclear Excitation

N. Tsoneva

Institut für Theoretische Physik, Universität Giessen
INRNE, Sofia, Bulgaria

in a collaboration with H. Lenske


Universität zu Köln

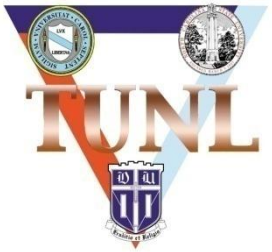

Sponsored by BMBF project 06GI9109

Characteristic Response of an Atomic Nucleus to EM Radiation

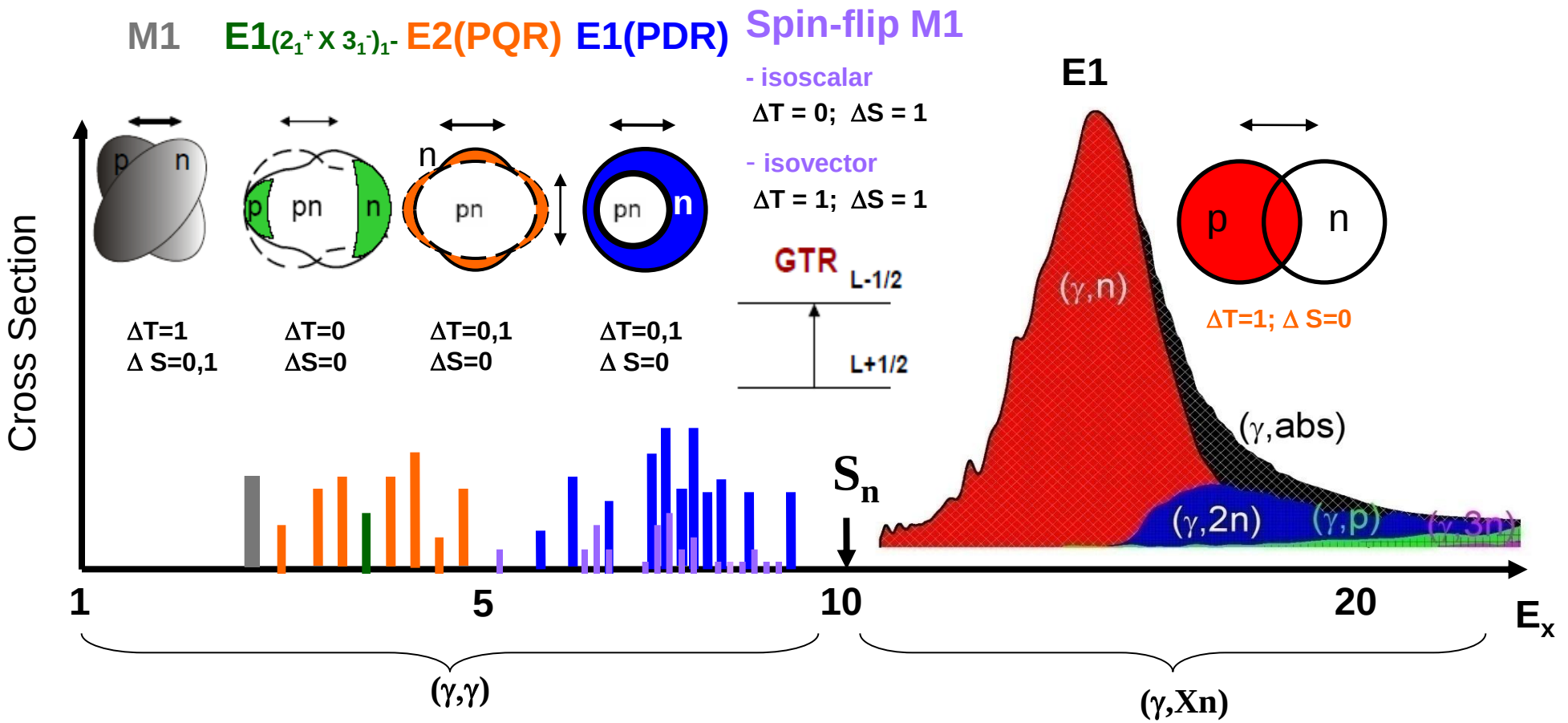

Moderate and Heavy nuclei :

- Orbital "Scissors" mode: E_x ~ 3 MeV, B(M1) ~ 3 μ_N^2
- Two Phonon Excitation: E_x ~ 4 MeV, B(E1) ~ 10^{-3} W.u.
- Pygmy Quadrupole Resonance: Ex ~ 2 - 5 MeV, B(E2) ~ 0.5 W.u.
- Pygmy Dipole Resonance: E_x ~ 6 - 9 MeV, B(E1) ~ 0.5 W.u.
- Spin-flip M1 excitations: E_x~ 4 - 12 MeV, B(E2) ~ 6 μ_N^2
- Giant Dipole Resonance: E_x ~ 10 - 20 MeV, B(E1) ~ 5 - 12 W.u.

Nucleosynthesis of Heavier Elements

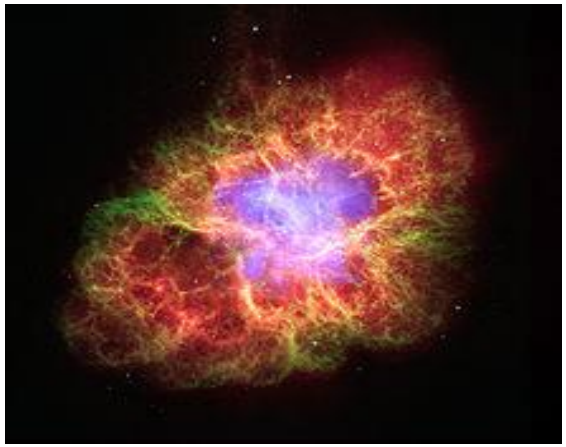

Heavier elements (Z> 26-28) can be assembled within stars by a neutron capture processes.

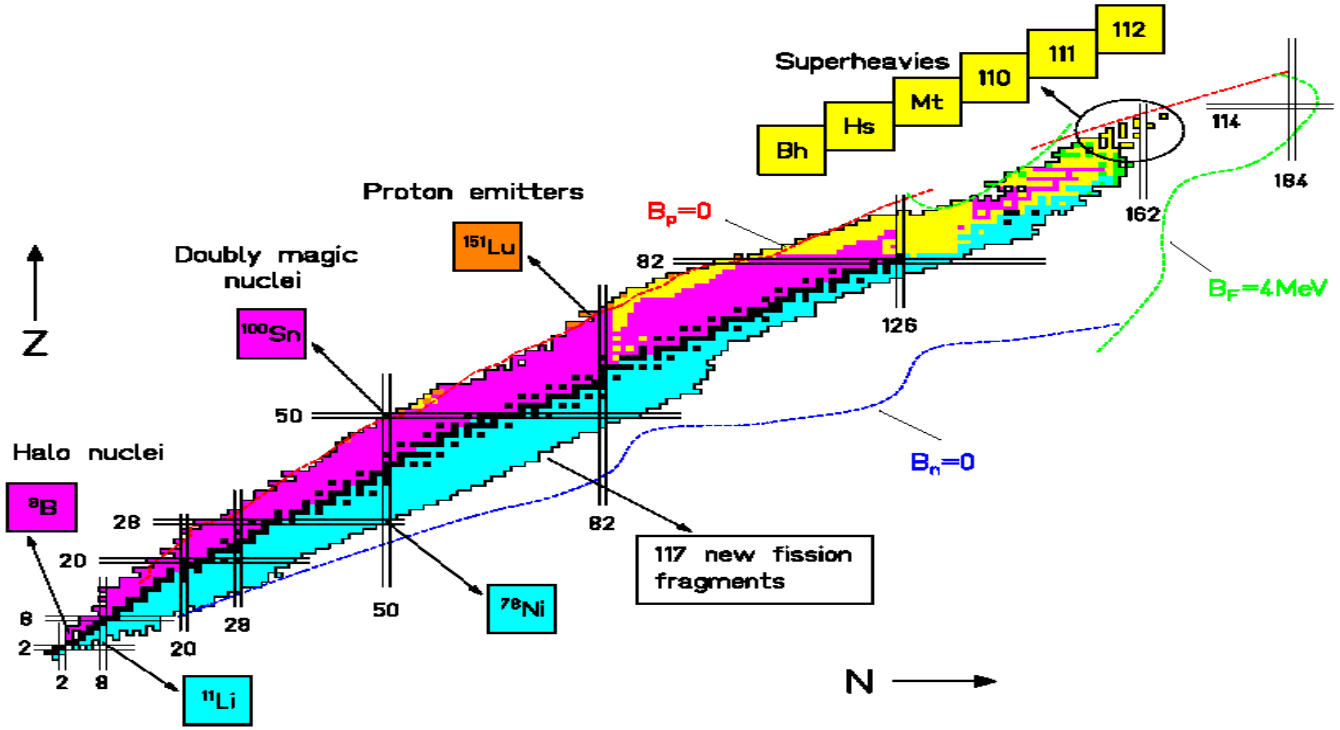

s- process – slow neutron capture,
low neutron densities
$\rho \sim 10^8/cm^3$
life time
$\tau \sim 1 – 10$ years

r – process - rapid neutron captures
$\rho \sim 10^{20}/cm^3$

ν – induced processes

rp – process - rapid proton captures

p-process (or γ-process) - photodisintegration of existing nuclei and ect…

Enhanced Dipole Strength

Observed dipole strength in stable nuclei with moderate neutron excess (N > Z)
below and close to the neutron-separation energy S_n
PDR ≤ 1% of the Thomas-Reiche-Kuhn sum rule (S_{TRK} ~ NZ/A)

Neutron PDR strength increases with the N/Z ratio !

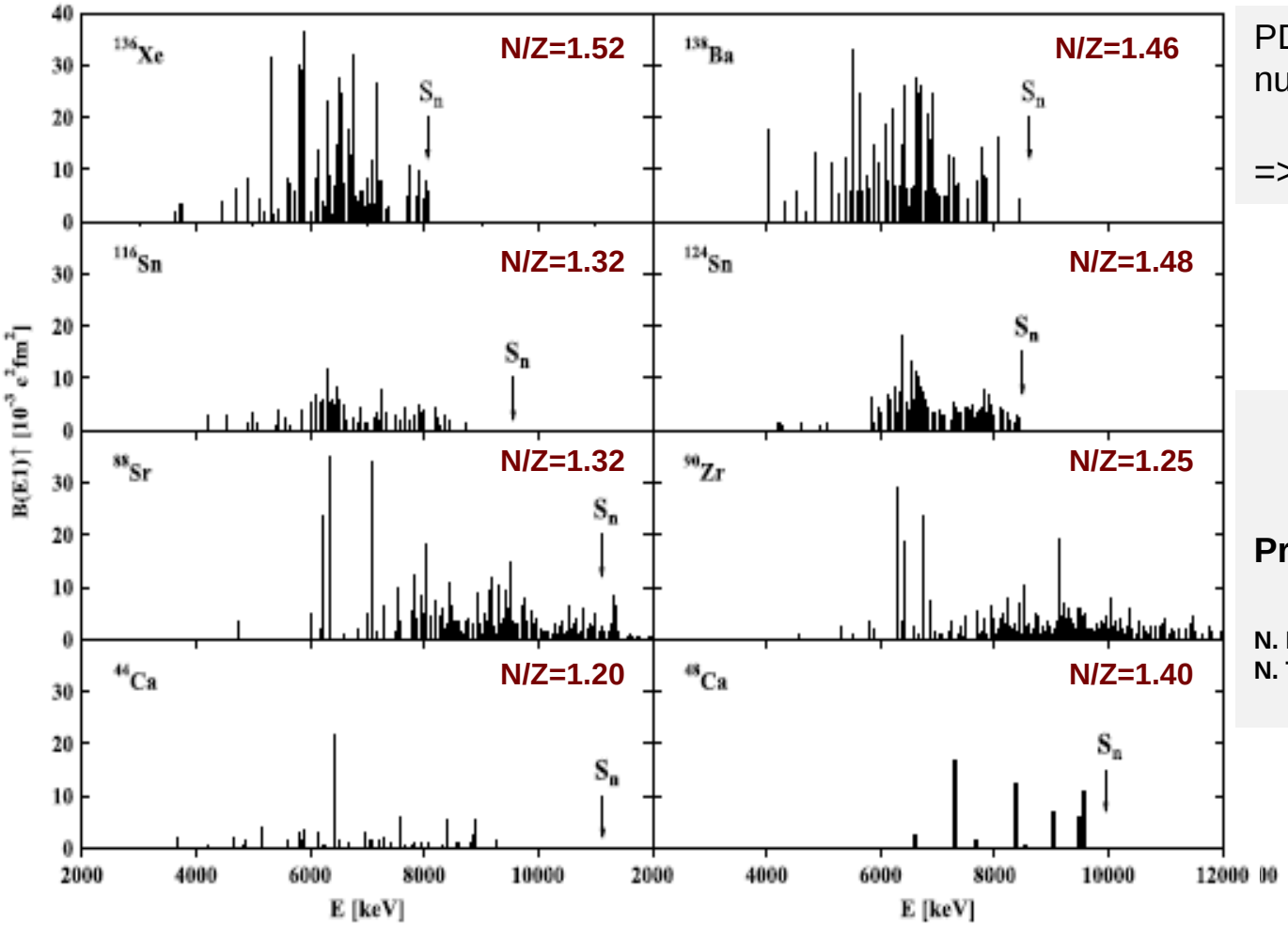

D. Savran et al. / Progress in Particle and Nuclear Physics 70 (2013) 210–245

PDR is independent of the type of nucleon excess (neutron or proton)

=> **Generic mode of excitation**

Proton PDR

Predicted in nuclei with Z ~ N

N. Paar et al. , PRL 94 (2005) 182501
N. Tsoneva et al., PRC 77 (2008) 024321

The Quasiparticle-Phonon Model

V. G. Soloviev: *Theory of Complex Nuclei* **(Pergamon Press, Oxford,1976)**

$$H = H_{MF} + H_{res}$$

$$H_{MF} = H_{sp} + H_{pair} \qquad H_{res} = H_M^{ph} + H_{SM}^{ph} + H_M^{pp}$$

Nuclear Ground State

Single-Particle States

Phenomenological density functional approach based on a fully microscopic self-consistent Hartree-Fock-Bogoljubov (HFB) theory

Pairing and Quasiparticle States

BCS gap equation, solved separately for protons and neutrons

Residual Interaction: Isoscalar and Isovector Separable Multipole-Multipole and Spin-Multipole intercations in the p-h and Multipole Pairing in the p-p channels;

The Multipole-Multipole interaction is given by:

$$V_\tau(|\vec{r} - \vec{r}\,'|) \approx \sum_{\lambda\mu} (-)^\mu R^\lambda(r,r') Y_{\lambda\mu}(\theta,\varphi) Y_{\lambda-\mu}(\theta',\varphi')$$

$$R^\lambda(r,r') = \kappa_\tau^\lambda R_\lambda(r) R_\lambda(r')$$

$$\kappa_\tau^\lambda = (\kappa_0^\lambda, \kappa_1^\lambda)$$

N. Tsoneva, H. Lenske, Ch. Stoyanov, Phys. Lett. B 586 (2004) 213
N. Tsoneva, H. Lenske, Phys. Rev. C 77 (2008) 024321

Phenomenological Density Functional Approach for Nuclear Ground States

P. Hohlenberg, W. Kohn, Phys. Rev. 136 (1964) B864; W. Kohn, L. J. Sham, Phys. Rev. 140 (1965) A 1133.

The total binding energy $B(A)$ can be expressed as an integral over an energy-density functional

$$B(A) = \sum_{q=p,n} \int d^3r \left(\tau_q(\rho) + \frac{1}{2}\rho_q U_q(\rho) \right) + E_q^{pair}(k,\rho)$$

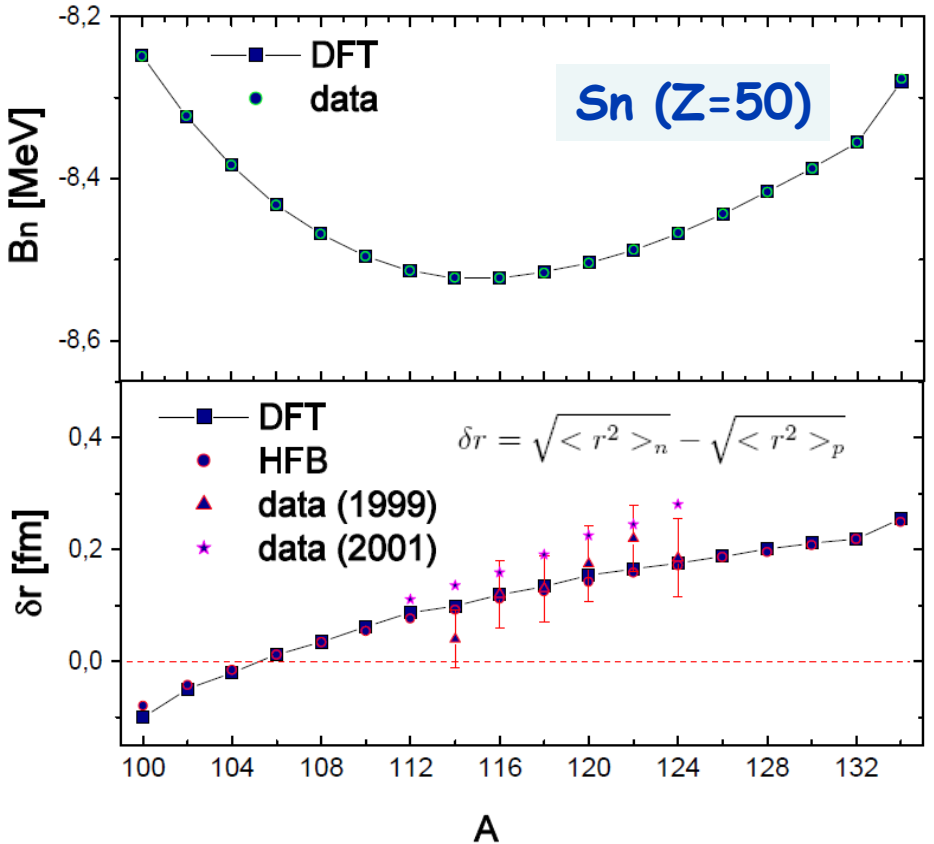

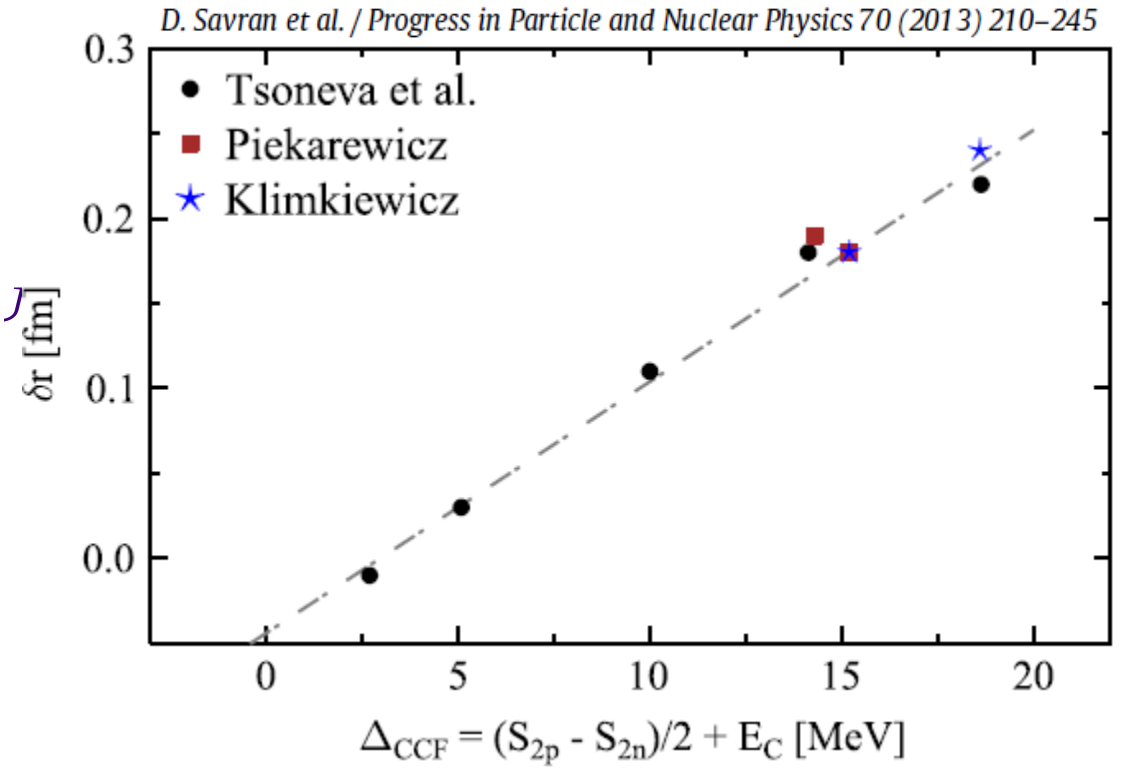

J

Calculations of Ground State Densities in Z=50, N=50,82 Nuclei

$$\rho_q(r) = \frac{1}{4\pi r^2} \sum_{\alpha_q} v^2_{\alpha_q} (2 j_{\alpha_q} + 1) R^2_{\alpha_q}(r)$$

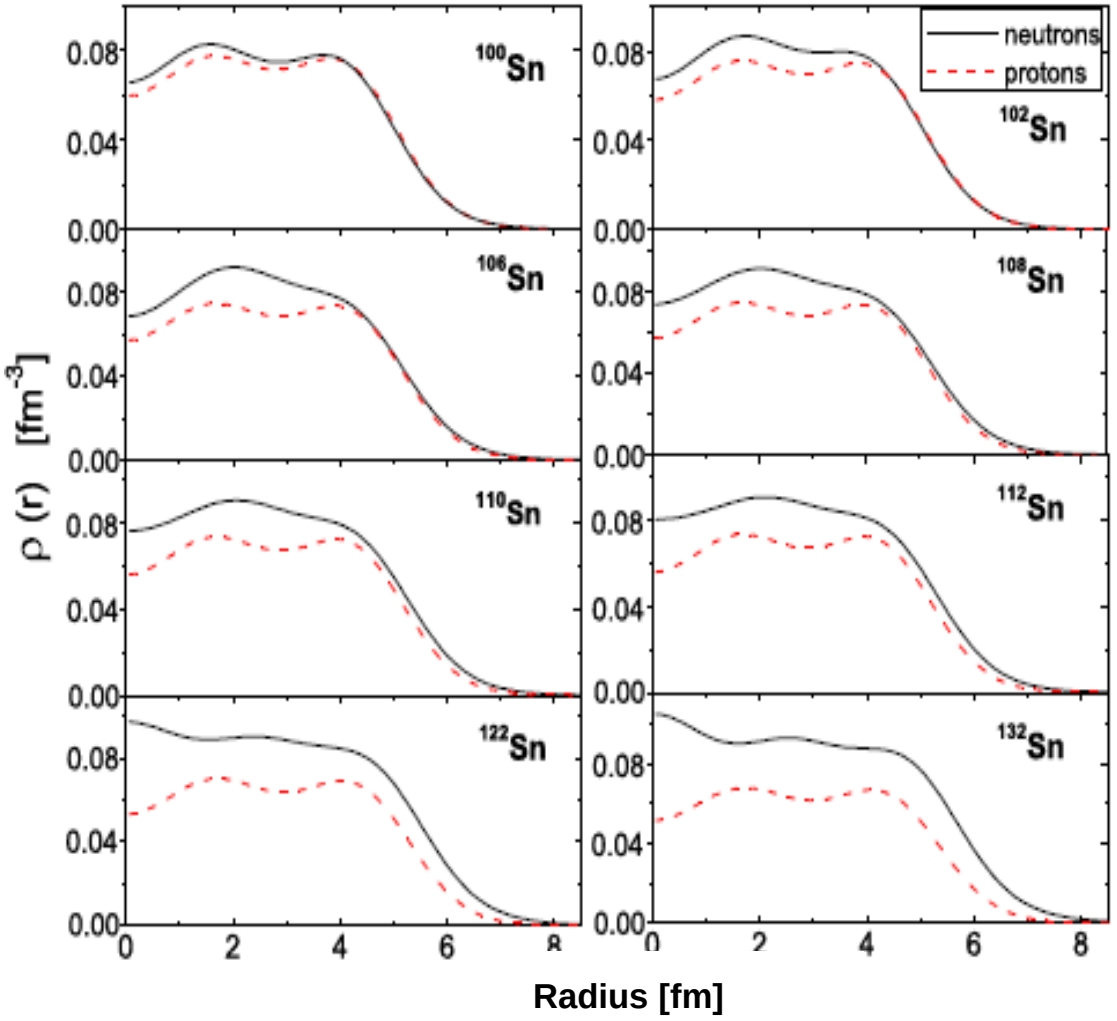

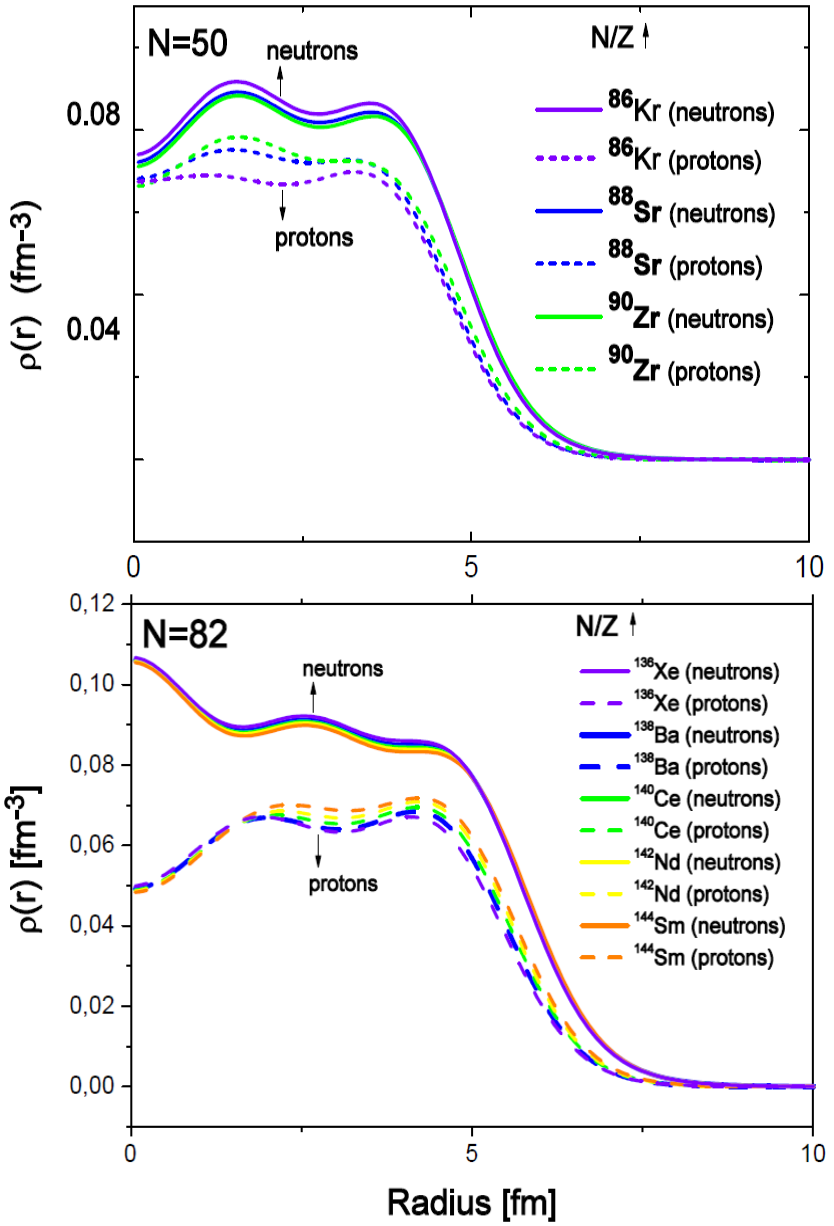

N. Tsoneva, H. Lenske, Phys. Rev. C 77 (2008) 024321
R. Schwengner et al., Phys. Rev. C 78 (2008) 064314

The Excited States

V. G. Soloviev: Theory of Atomic Nuclei: *Quasiparticles and Phonons* **(Inst. Of Phys. Publ., Bristol, 1992)**

$$Q^+_{\lambda\mu i} = \frac{1}{2}\sum_{\tau}^{n,p}\sum_{jj'}\left\{\psi^{\lambda i}_{jj'}[\alpha^+_j\alpha^+_{j'}]_{\lambda\mu} - (-1)^{\lambda-\mu}\varphi^{\lambda i}_{jj'}[\alpha_{j'}\alpha_j]_{\lambda-\mu}\right\} ,$$

$$a_{jm} = u_j\alpha_{jm} + (-)^{j-m}v_j\alpha^+_{j-m}$$

$$[Q_{\lambda\mu i}, Q^+_{\lambda'\mu' i'}] = \frac{\delta_{\lambda,\lambda'}\delta_{\mu,\mu'}\delta_{i,i'}}{2}\sum_{jj'}[\psi^{\lambda i}_{jj'}\psi^{\lambda i'}_{jj'} - \varphi^{\lambda i}_{jj'}\varphi^{\lambda i'}_{jj'}] - \sum_{\substack{jj'j_2\\ mm'm_2}} \boxed{\alpha^+_{jm}\alpha_{j'm'}}$$

$$\times\left\{\psi^{\lambda i}_{j'j_2}\psi^{\lambda' i'}_{jj_2}C^{\lambda\mu}_{j'm'j_2m_2}C^{\lambda'\mu'}_{jmj_2m_2} - (-)^{\lambda+\lambda'+\mu+\mu'}\varphi^{\lambda i}_{jj_2}\varphi^{\lambda' i'}_{j'j_2}C^{\lambda-\mu}_{jmj_2m_2}C^{\lambda'-\mu'}_{j'm'j_2m_2}\right\}$$

$$\left[H, Q^+_\alpha\right] = E_\alpha Q^+_\alpha$$

The Wave Function

For even-even nucleus the QPM wave functions are a mixture of one-, two- and three-phonon components

$$\Psi_\nu(JM) = \Bigg\{ \sum_i R_i(J\nu) Q^+_{JMi} + \sum_{\substack{\lambda_1 i_1 \\ \lambda_2 i_2}} P^{\lambda_1 i_1}_{\lambda_2 i_2}(J\nu) \left[Q^+_{\lambda_1 \mu_1 i_1} \times Q^+_{\lambda_2 \mu_2 i_2} \right]_{JM}$$

$$+ \sum_{\substack{\lambda_1 i_1 \lambda_2 i_2 \\ \lambda_3 i_3 I}} T^{\lambda_1 i_1 \lambda_2 i_2 I}_{\lambda_3 i_3}(J\nu) \left[\left[Q^+_{\lambda_1 \mu_1 i_1} \otimes Q^+_{\lambda_2 \mu_2 i_2} \right]_{IK} \otimes Q^+_{\lambda_3 \mu_3 i_3} \right]_{JM} \Bigg\} \Psi_0$$

M. Grinberg, Ch. Stoyanov, Nucl. Phys. A. 573 (1994) 231

QRPA Calculations on the Dipole Response in Sn Isotopes

A connection between the total PDR strength and the neutron or proton skin

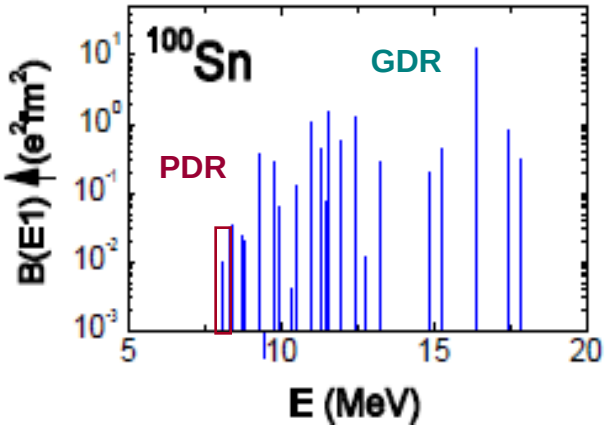

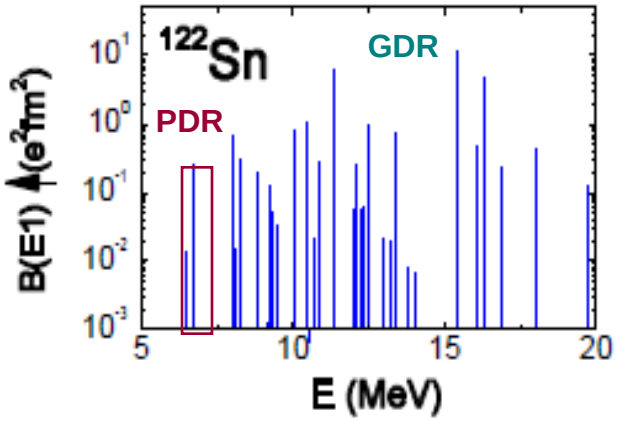

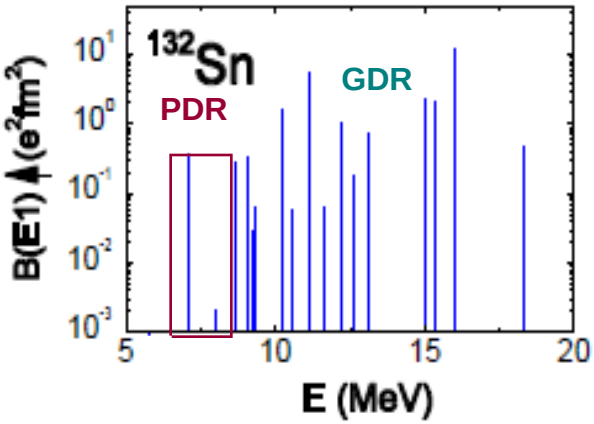

Dipole Transition Densities in Sn Isotopes

N.Tsoneva, H. Lenske, PRC 77 (2008) 024321

Transition densities are directly related to nuclear response functions

$$\delta\rho^{T}(\vec{r}) = \sum_{j_1 j_2;\lambda\mu} [i^{\lambda} Y_{\lambda\mu}(\hat{r})]^{\dagger} \rho^{\lambda T}_{j_1 j_2}(r) \left[a^{+}_{j_1} a_{j_2}\right]_{\lambda\mu}.$$

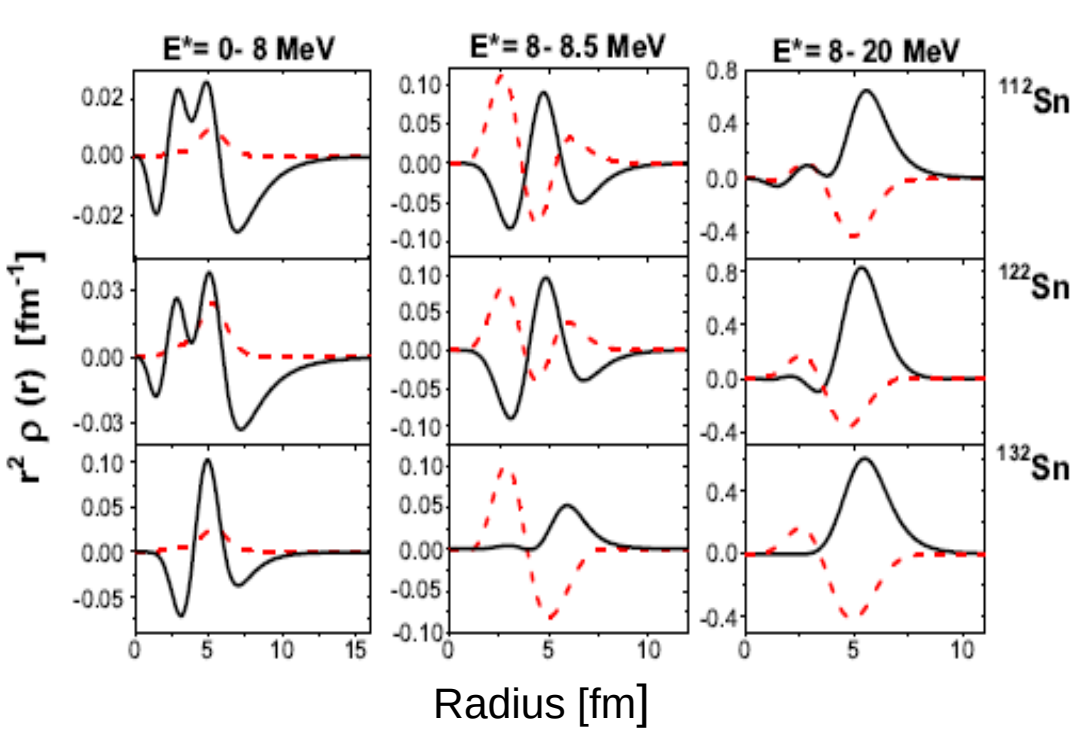

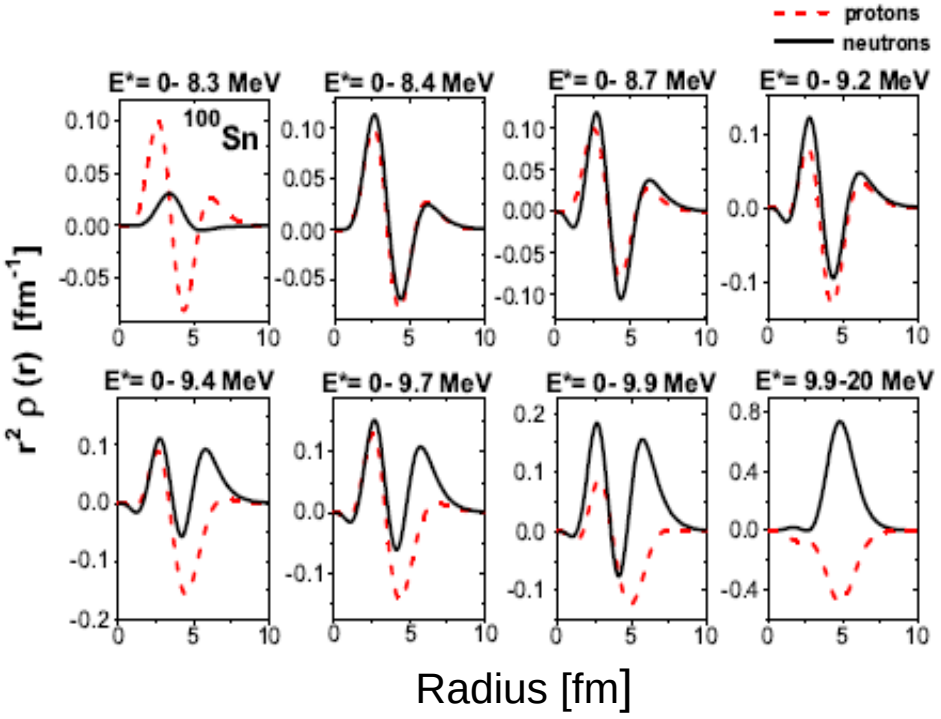

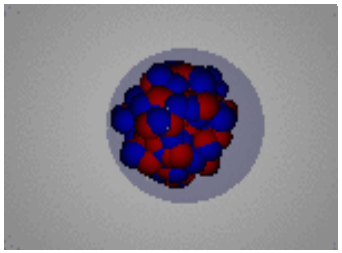

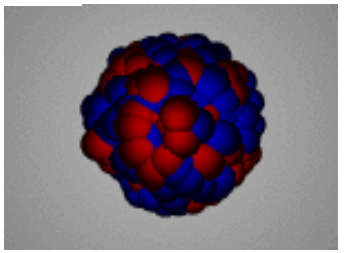

Skin Thickness and Electric Dipole Response

N. Tsoneva, H. Lenske, Ch. Stoyanov, Phys. Lett. B 586 (2004) 213; N. Tsoneva, H. Lenske, PRC 77 (2008) 024321

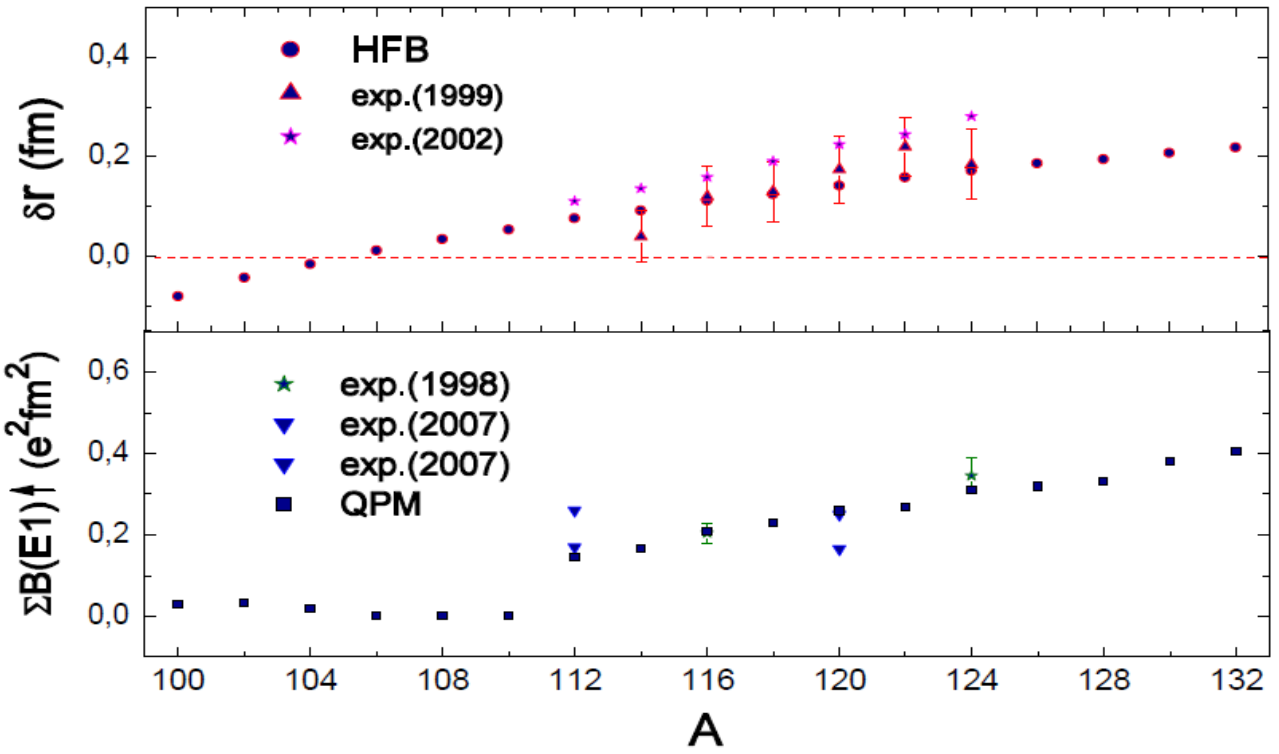

Neutron skin thickness increases with increasing neutron number ;

$$\delta r = \sqrt{\langle r_n^2 \rangle} - \sqrt{\langle r_p^2 \rangle},$$

PDR strength increases with increasing neutron skin thickness !

$$\Delta_3 r^2 = \sum_i \langle 0 | \tau_{3i} r_i^2 | 0 \rangle,$$

$$\Delta_3 r^2 = \frac{1}{4 q_0 q_1} \left(\sum_d B_d(E1) - q_0^2 \sum_d \left| M_d^{(0)} \right|^2 - q_1^2 \sum_d \left| M_d^{(1)} \right|^2 \right)$$

+ ground state pairing correlations

$$B_d(E1) = \left| q_0 \vec{M}_d^{(0)} + q_1 \vec{M}_d^{(1)} \right|^2 \qquad q_T = \frac{1}{2}(q_n + (-)^T q_p); \quad \vec{M}_d^{(T)} = \langle 0 \| (\tau_3)^T \vec{r} \ \| d \rangle;$$

Boson Forbidden Transitions

$$\left\langle Q_{\lambda_N i_N} \ldots Q_{\lambda_2 i_2} Q_{\lambda_1 i_1} \left\| M(E\lambda) \right\| Q^+_{\lambda i} Q^+_{\lambda_1 i_1} Q^+_{\lambda_2 i_2} \ldots Q^+_{\lambda_N i_N} \right\rangle \neq 0$$

QRPA

$$M(E(M)_{\lambda\mu} = M^{Ph} + M^{QPh}(E(M)_{\lambda\mu})$$

$$\approx \left[\alpha^+_j \otimes \alpha^+_{j'} \right]$$

QPM

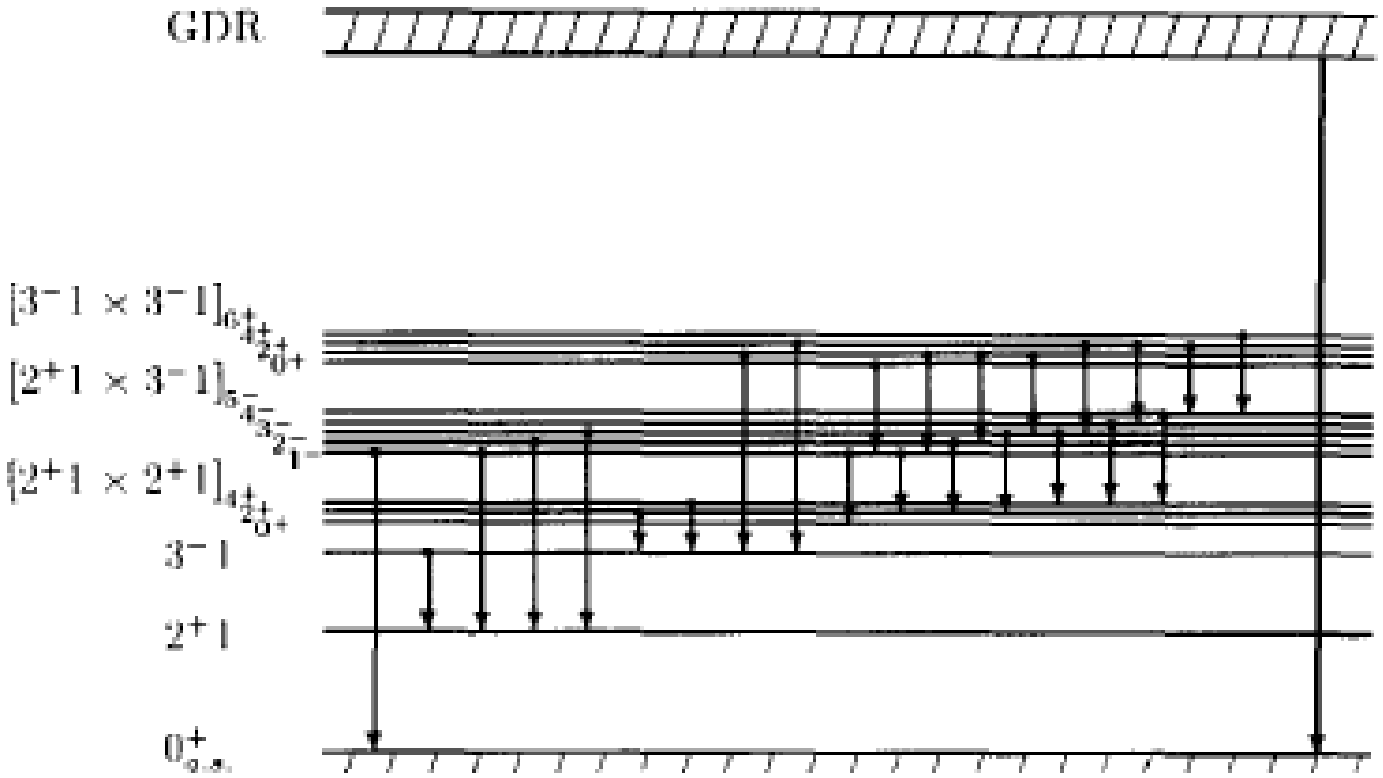

V. Ponomarev, Ch.Stoyanov, N. Tsoneva, M. Grinberg, Nucl. Phys. A 635 (1998) 470

Multiphonon Calculations of E1 Transitions in ^{112,120}Sn

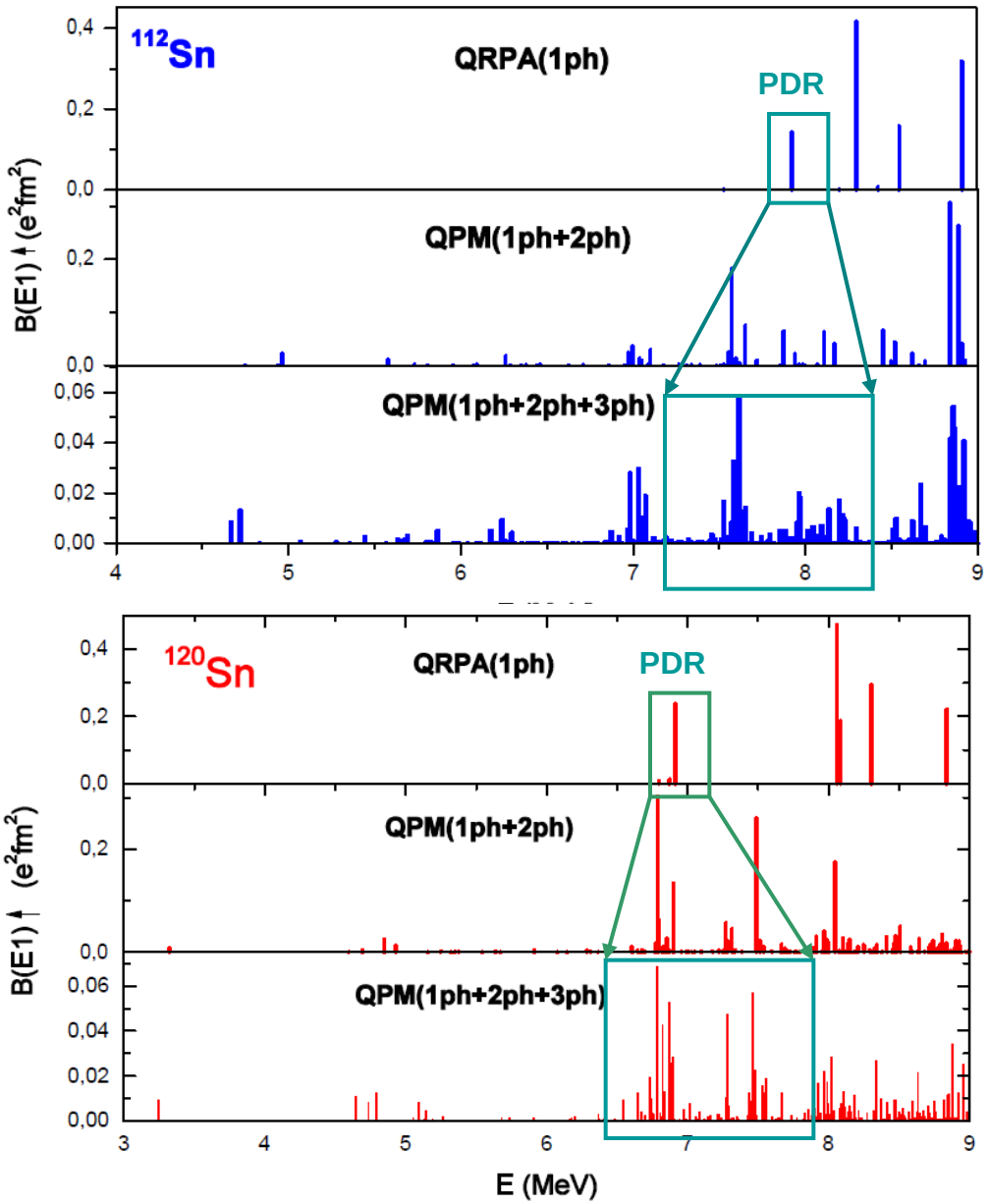

N/Z(^{112}Sn)= 1.24

N/Z(^{120}Sn)= 1.4

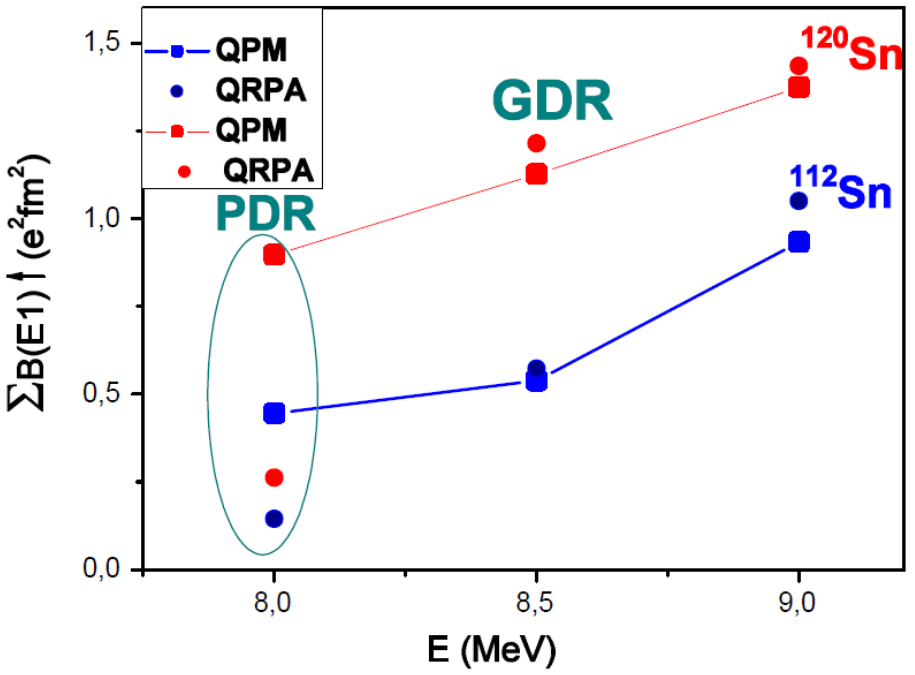

GDR (E*>8MeV) (1ph)

PDR (1ph+2ph+3ph)

Theoretical Prediction of Pygmy Quadrupole Resonance

QRPA Calculations of Isoscalar and Isovector Quadrupole States up to 35 MeV in Sn Isotopes

$$M_I(2^+) \approx \langle 2^+ \| \sum_k^A r_k^2 Y_{2\mu}(\Omega_k)(\tau_3)^I \| \text{g.s.} \rangle$$

N. Tsoneva, H. Lenske, Phys. Lett. B 695 (2011) 174

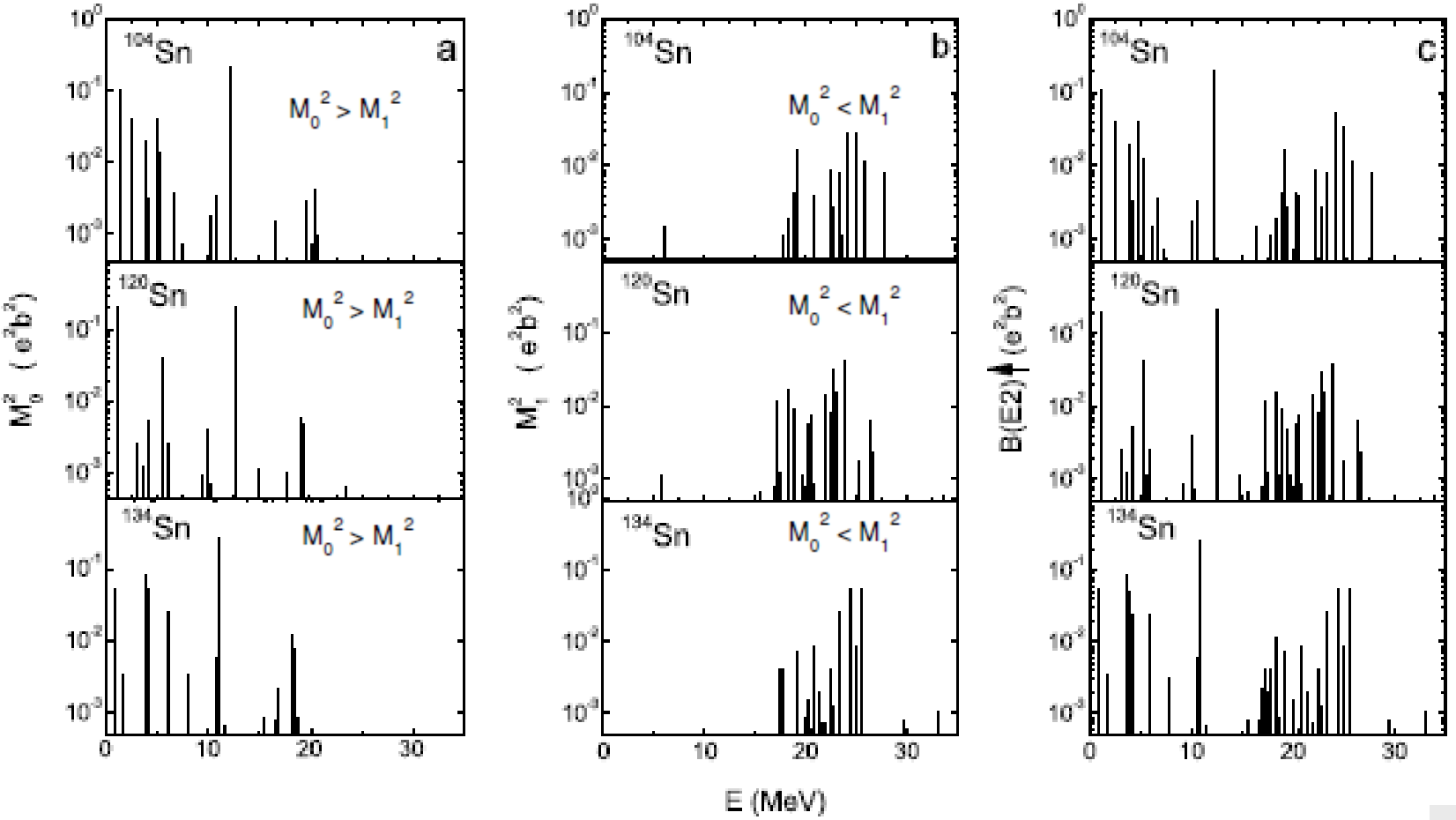

Quadrupole Transition Densities in Sn Isotopes

A Signature of Pygmy Quadrupole Resonance

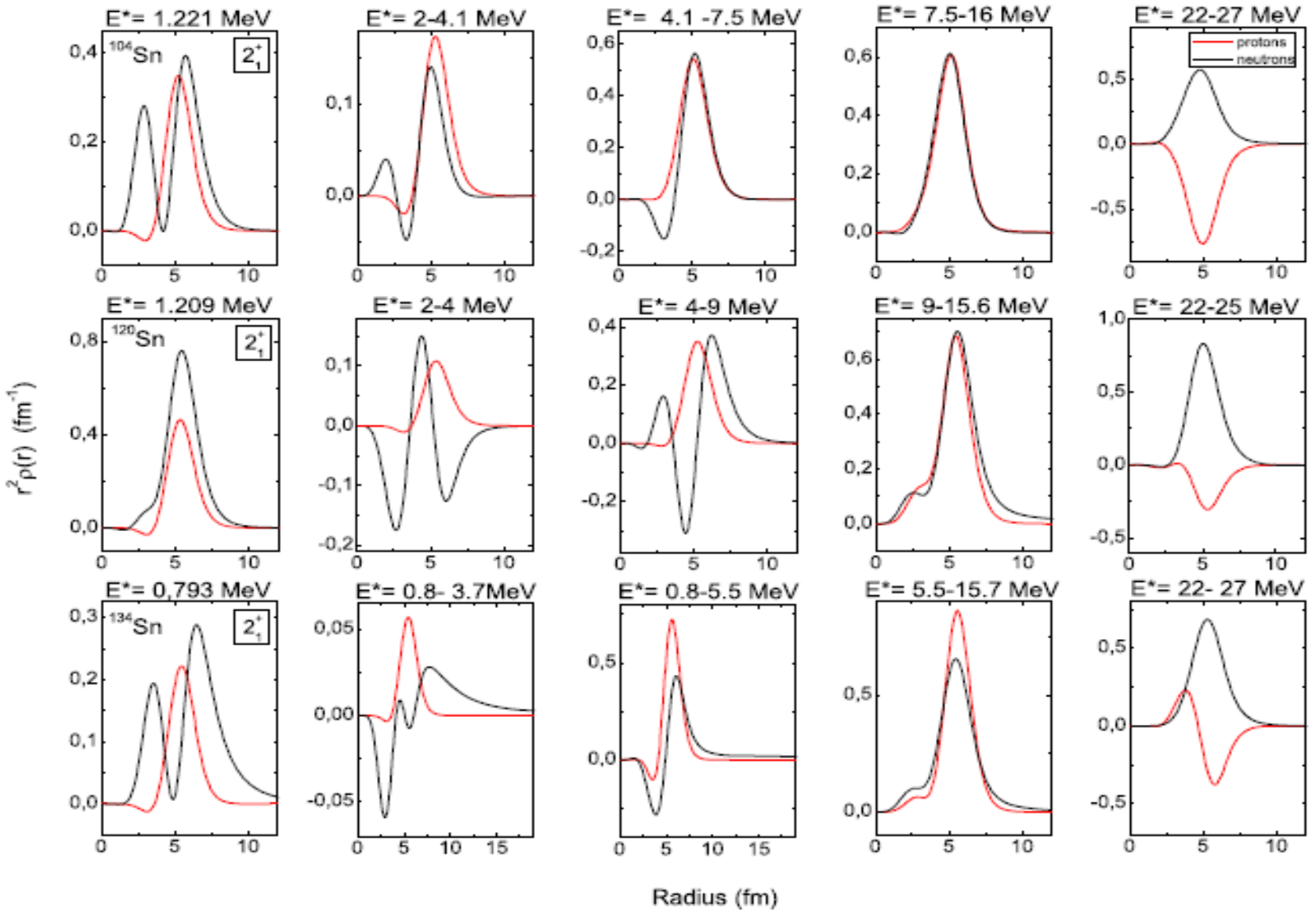

QRPA Calculations of Low-Energy 2^+ States Related to PQR

N. Tsoneva and H. Lenske, Phys. Lett. B 695, 174 (2011)

Pygmy quadrupole resonance is a genuine mode!

B(M1) to the first symmetric $2_1^+ \sim 10^{-2}\mu_N^2$

B(E2) increases with the neutron number,

B(E2) ~ 1/ ε_b ^{2}

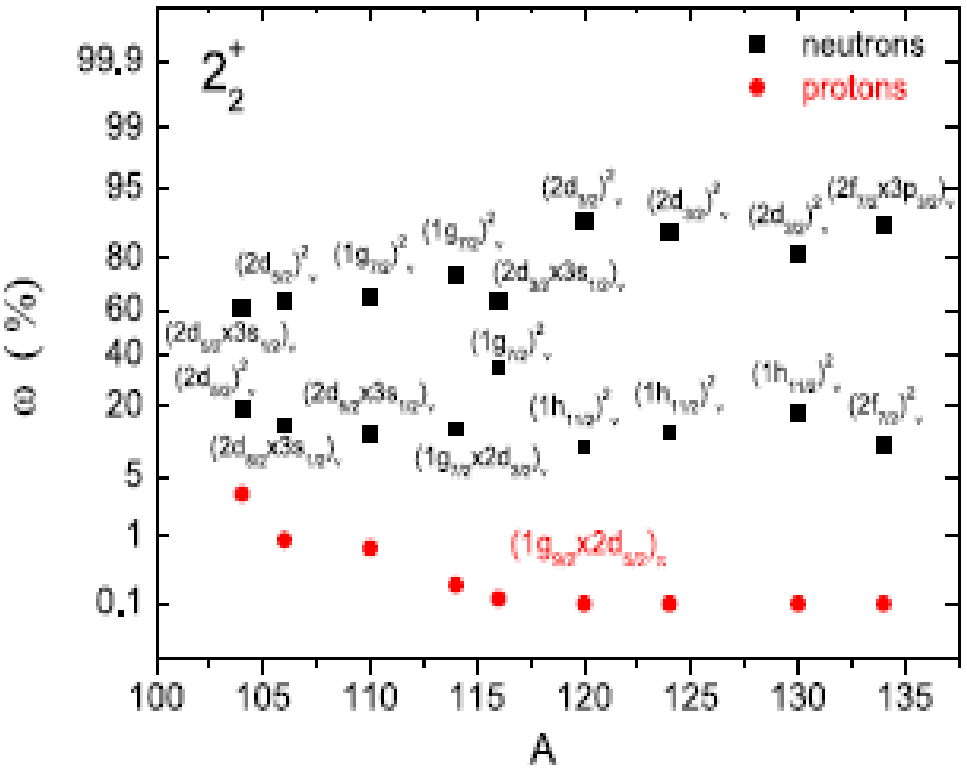

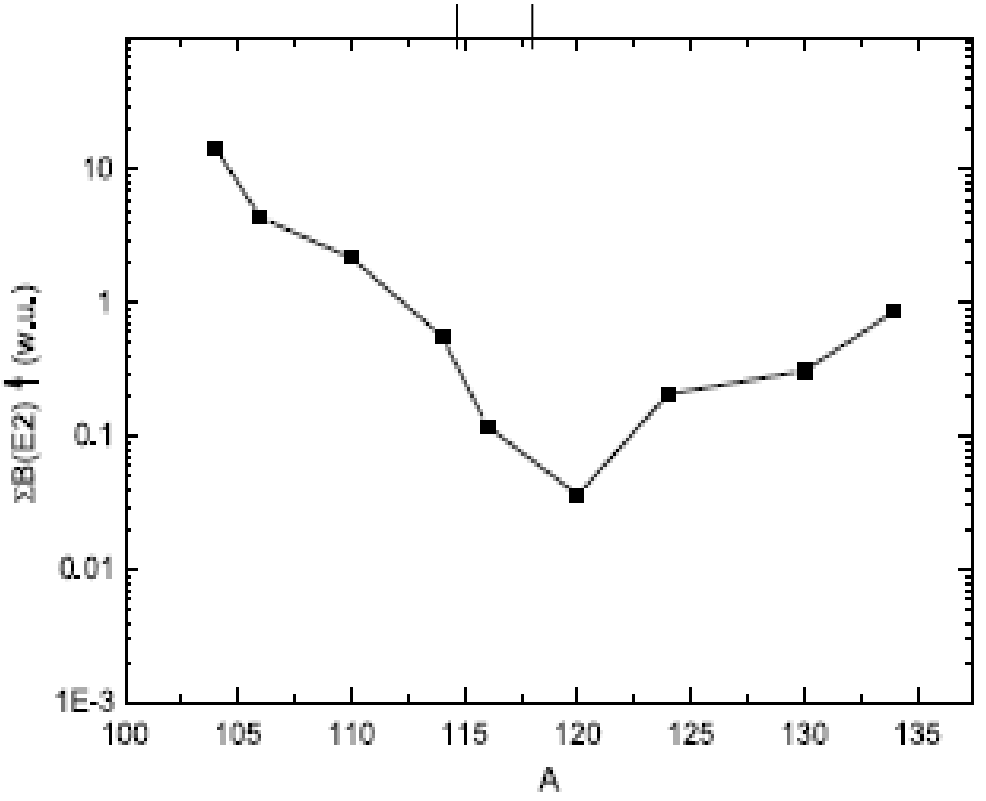

A change in the E_b of the $g_{9/2}$ which is the proton Fermi level in Sn isotopes when approaching the N=Z limit.

E_b= -12.88 MeV in ^{134}Sn ; E_b=-7.20 MeV in ^{104}Sn

QPM Calculations of PQR Strength in Comparison with (γ,γ') Data

M. Spieker, J. Enders, A. Zilges, Universität zu Köln, private communication)

J. Bryssinck et al., Phys. Rev. C 61 024309 (2000);

National Nuclear Data Center; Nucl. Data Scheets 109 (2008) 18668.

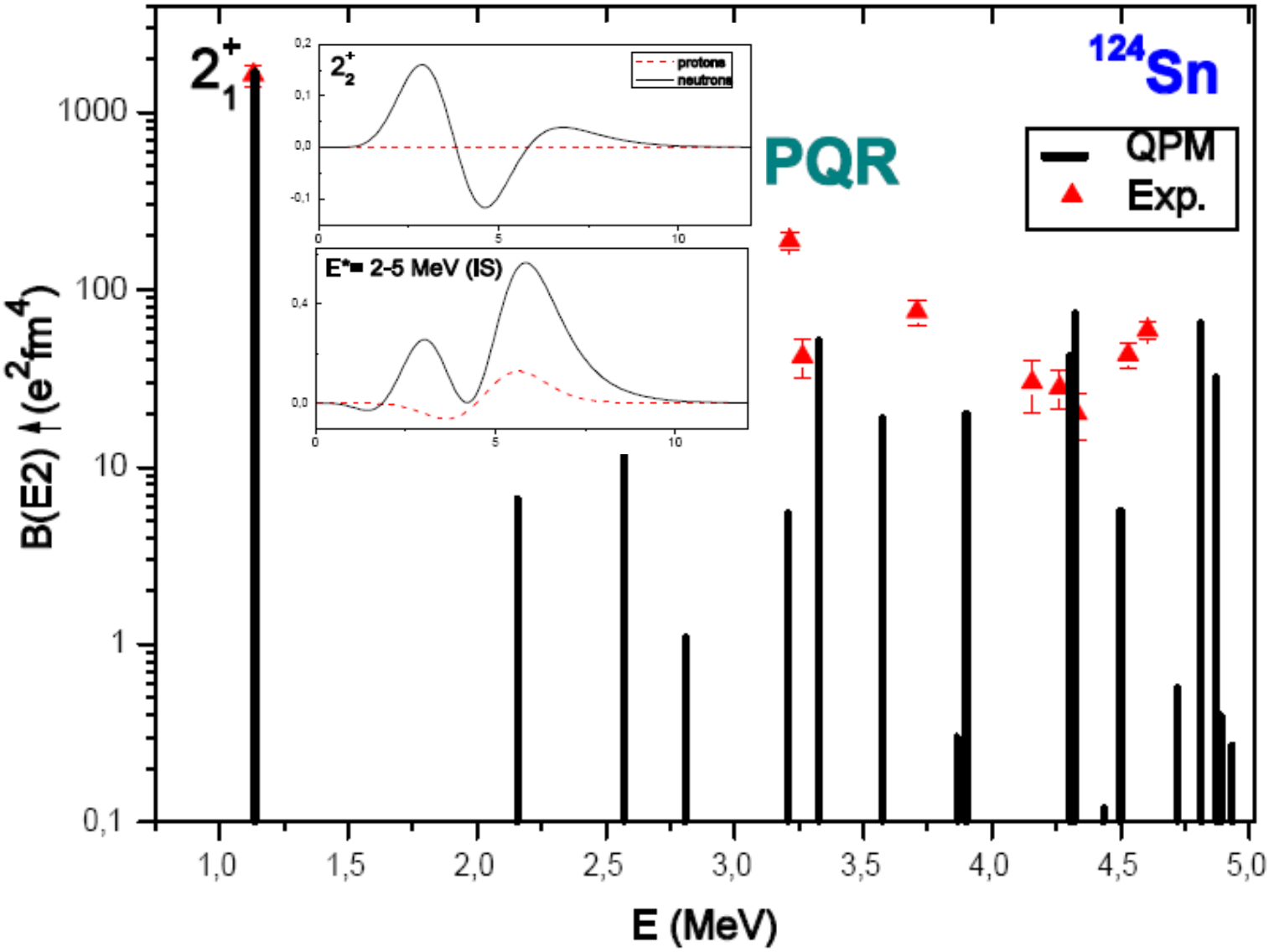

$$\sum_{2MeV}^{5MeV} B(E2)^{\text{exp.}} \uparrow = 489 e^2\, fm^4$$

$$\sum_{2MeV}^{5MeV} B(E2)^{QPM} \uparrow = 341 e^2\, fm^4$$

B(E2) in $^{32}Mg/^{34}Mg$ and $^{33}Al/^{35}Al$ (QRPA): Spectral Distribution normalized to EWSR

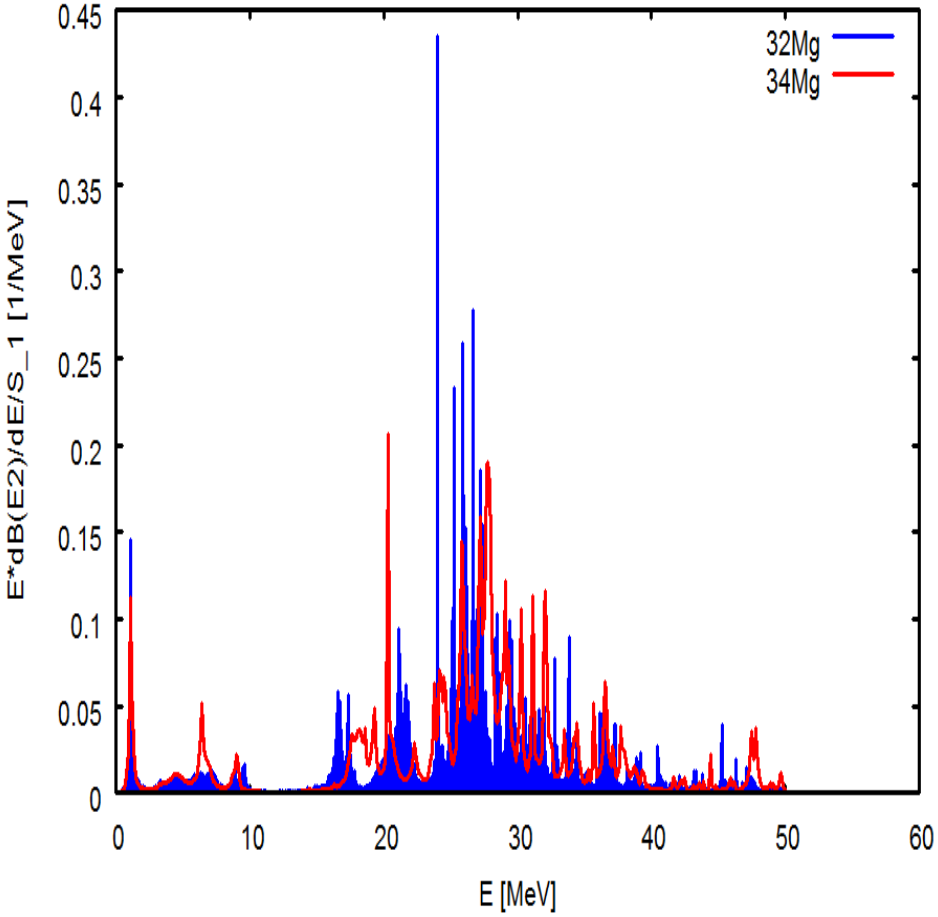

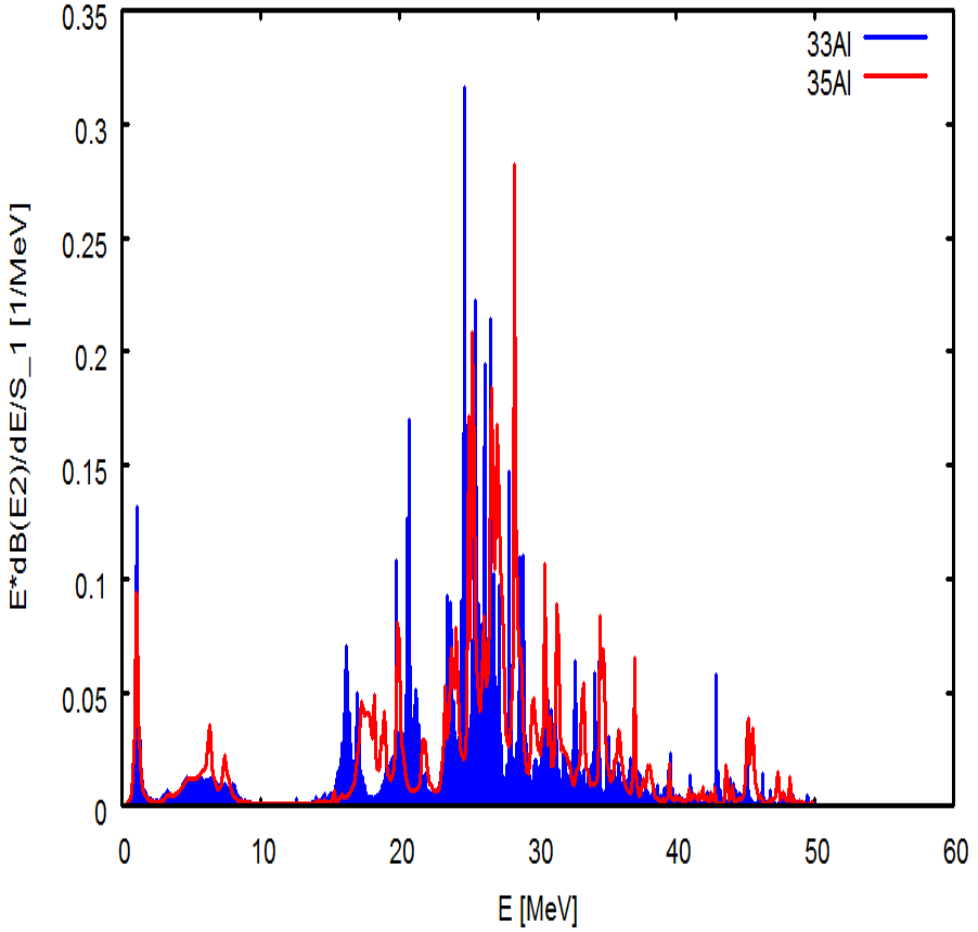

Parity Measurements with Polarized Photon Beams of Low-energy Dipole Excitations at HIγS, Duke University

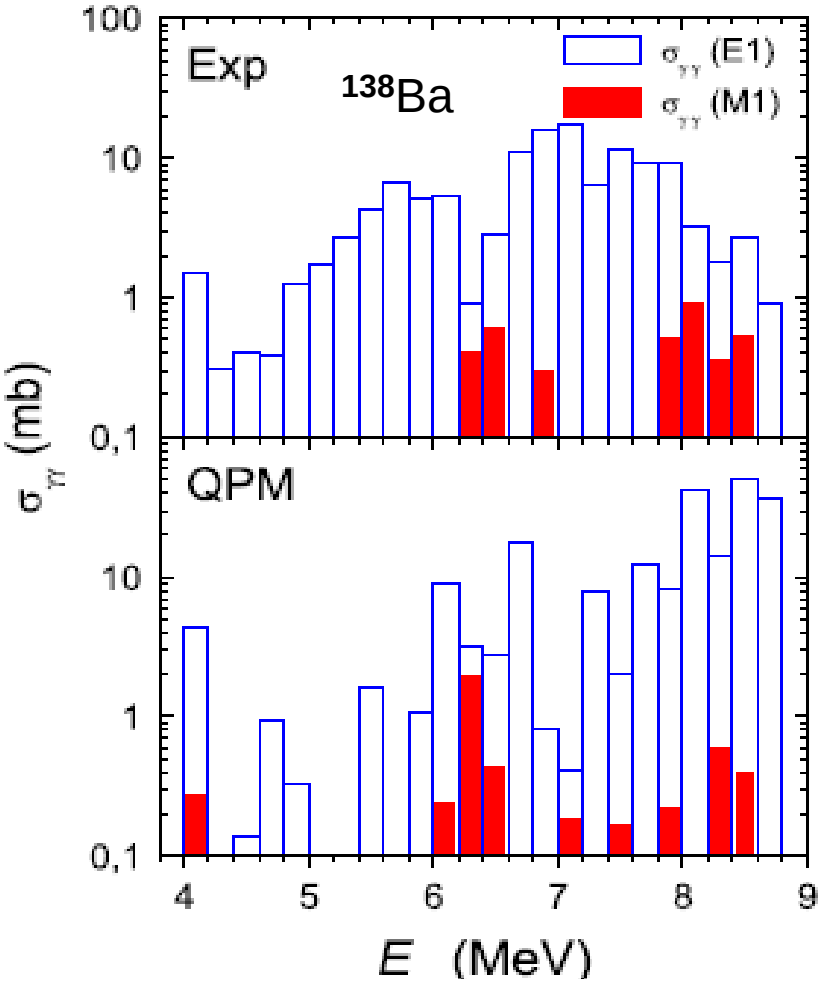

A. Tonchev et al., Phys. Rev. Lett. 104, 072501 (2010)

$\sigma_{\gamma\gamma}(M1)/\sigma_{\gamma\gamma}(E1)$ ~ 3%

- First systematic spin and parity measurements and the QPM calculations ^{138}Ba verified for the first time that the observed dipole strength from 4~MeV to particle separation energy is predominantly electric dipole in nature and it could be related to pygmy dipole resonance and neutron skin oscillations.
- The fine structure of the M1 spin-flip mode was observed and theoretically described for the first time in N = 82 nuclei.
- Separation of the PDR to isoscalar and isovector. Interplay between the GDR and the PDR at higher energies. As the excitation energy increases, the isovector contribution to the dipole strength exponentially increases due to the left tail of the GDR.

TABLE I. $E1$ and $M1$ parameters deduced in ^{138}Ba below the neutron-separation energy in comparison with the QPM calculations.

	$\langle E_{E1}\rangle$ [MeV]	$\Sigma B(E1)\uparrow$ [e^2 fm^2]	$\langle E_{M1}\rangle$ [MeV]	$\Sigma B(M1)\uparrow$ [μ_N^2]	EWSR$_{E1}$ [%]
Experimental	6.7	0.96(18)	6.9	2.5(6)	1.3
QPM	7.3	1.22	6.9[a]	2.9[a]	1.8

[a] 4.1 MeV $< E^* <$ 8.5 MeV.

Fine Structure of the Giant M1 Resonance in ^{90}Zr

The theory observes increased contribution of the orbital magnetic moment.
The effect is estimated to account for about 22% of the total M1 strength below the threshold.

G. Rusev, N. Tsoneva, F. Dönau, S. Frauendorf, R. Schwengner, A. P. Tonchev, A. S. Adekola, S. L. Hammond, J. H. Kelley, E. Kwan, H. Lenske, W. Tornow, and A. Wagner
Phys. Rev. Lett. 110, 022503 (2013)

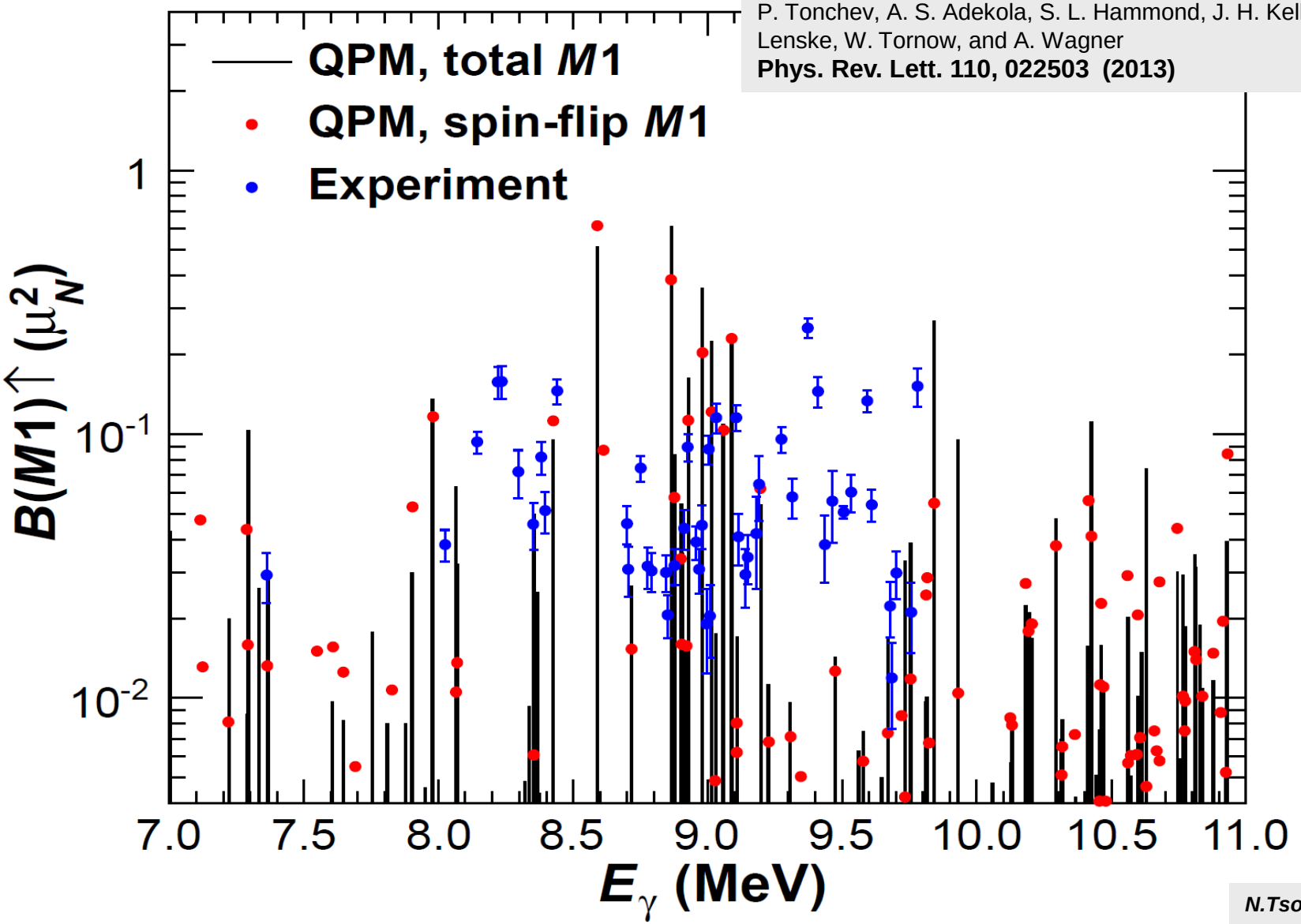

Comparison of 3-phonon QPM calculations and experiment on the values of total measured M1 strength and its centroid energy in the energy range E*=7-11 MeV

G. Rusev et al., Phys. Rev. Lett. 110, 022503 (2013)

$\Sigma B(M1)_{Exp.}$ = 4.5 (6) μ_N^2 ; $E^{c.m.}{}_{Exp.}$ = 9.0 MeV

$\Sigma B(M1)_{QPM.}$ = 4.6 μ_N^2 ; $E^{c.m.}{}_{QPM}$ = 9.1 MeV

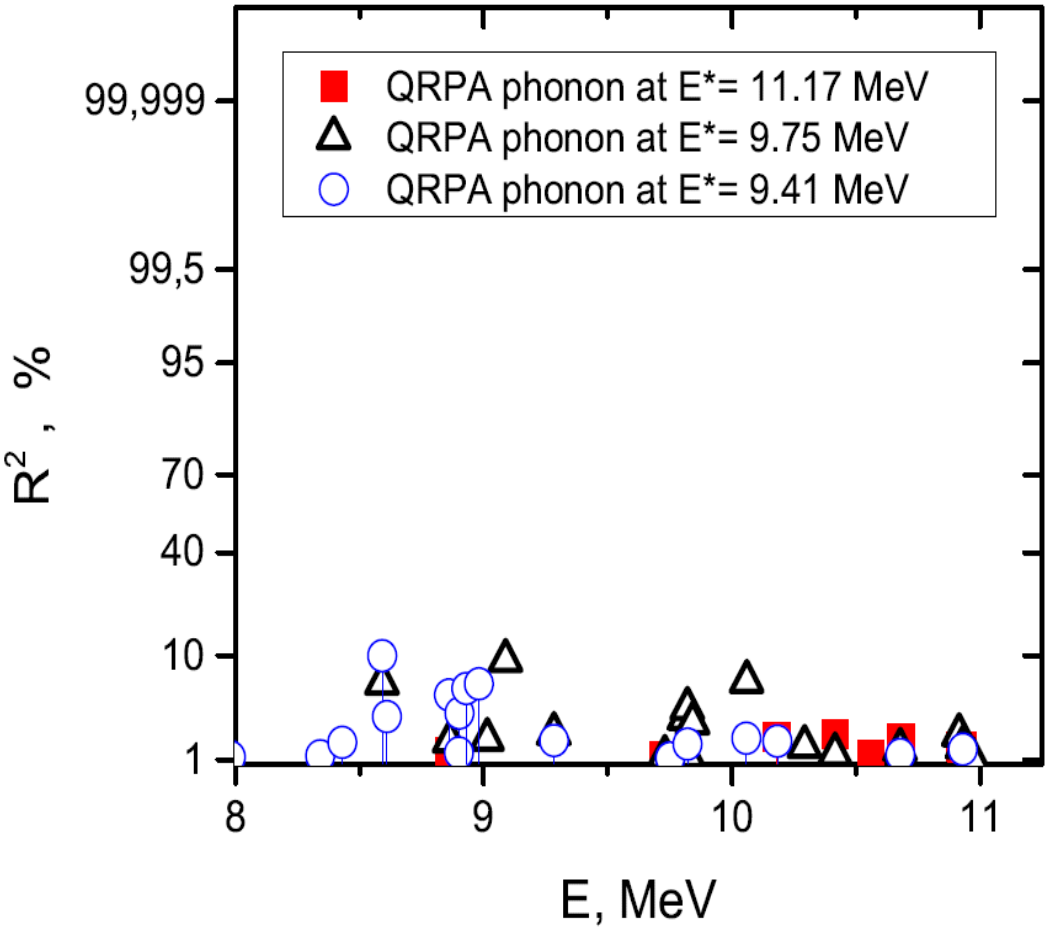

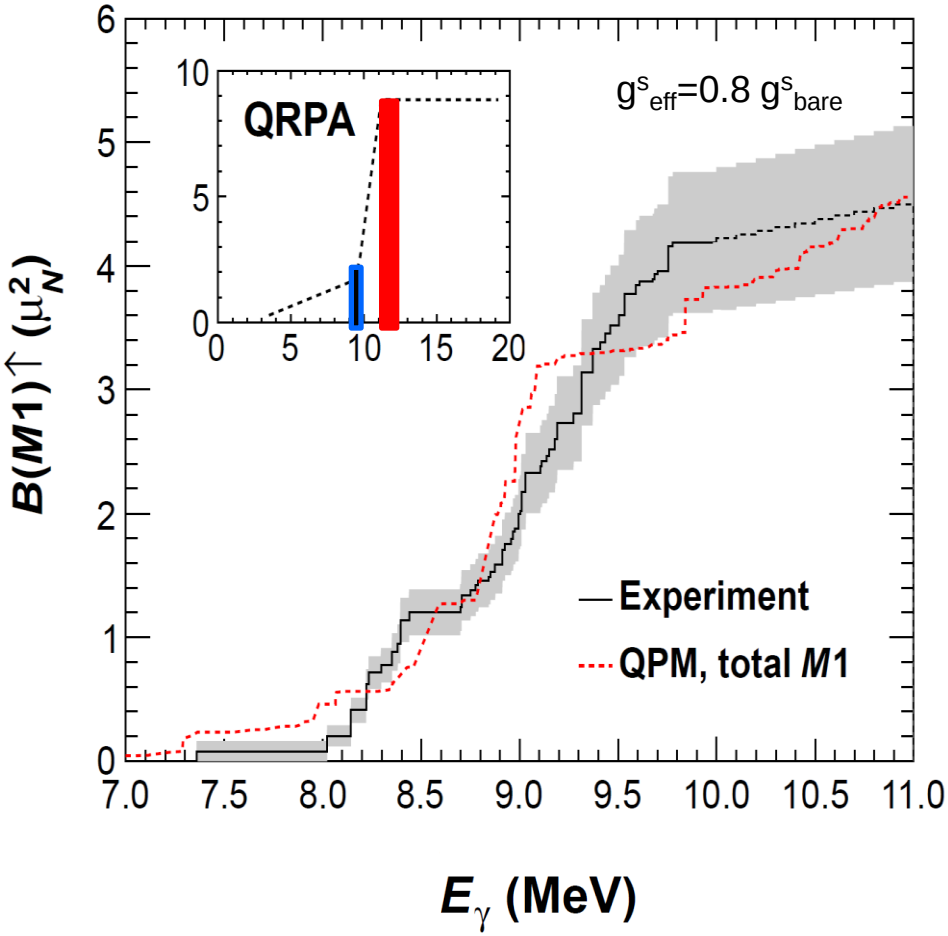

QPM Predictions of M1 Strength around and above the Neutron Threshold

first confirmations from (p, p') experiment (C. Iwamoto et al., Phys. Rev. Lett. 108, 262501 (2012))

Explaining the fragmentation pattern and the dynamics of the 'quenching' means to understand the coupling of the 2-QP doorway states to many-QP configurations

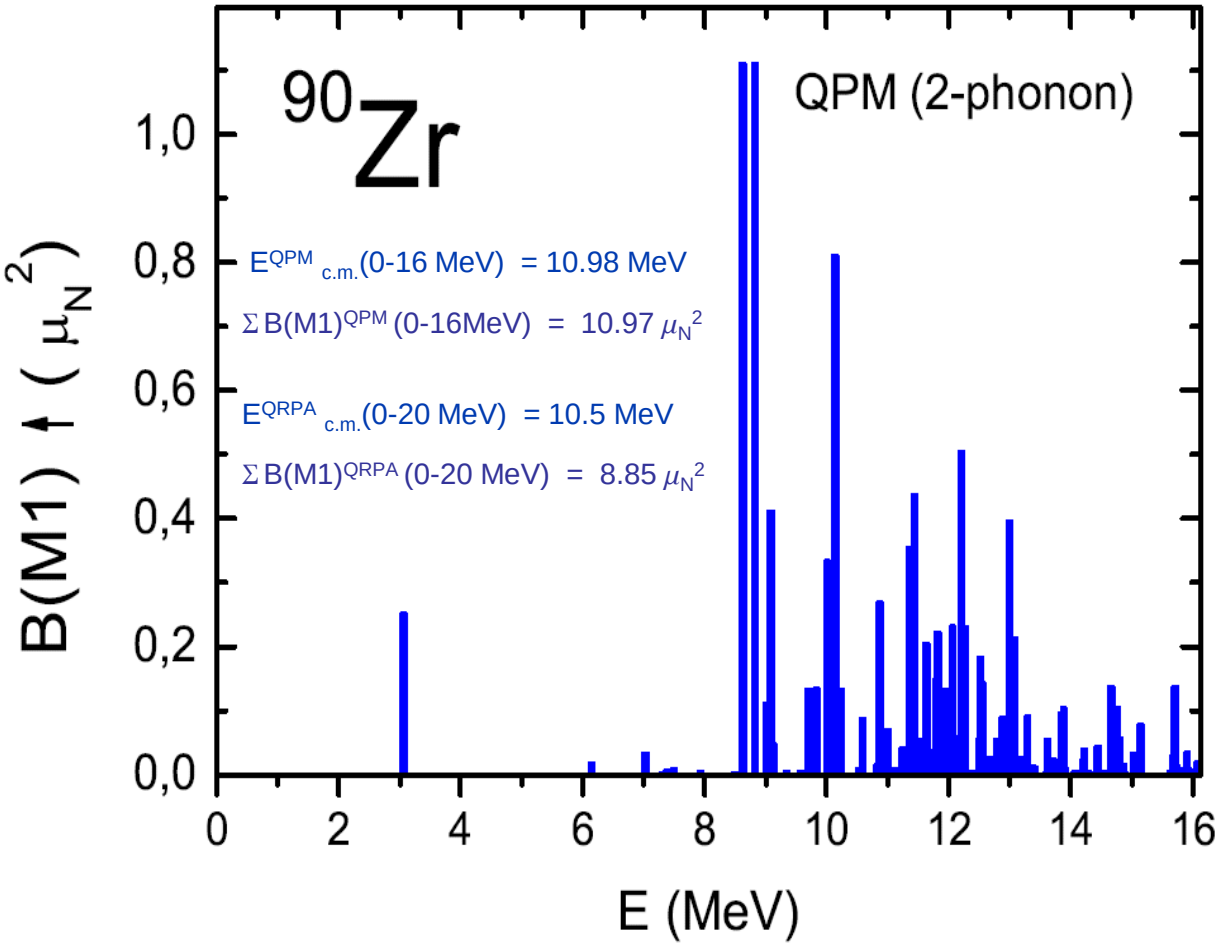

$E^{QPM}_{c.m.}$ (6-12 MeV) = 9,6 MeV

$E^{exp}_{c.m.}$ (6-12 MeV) = 9,53(0.06) MeV

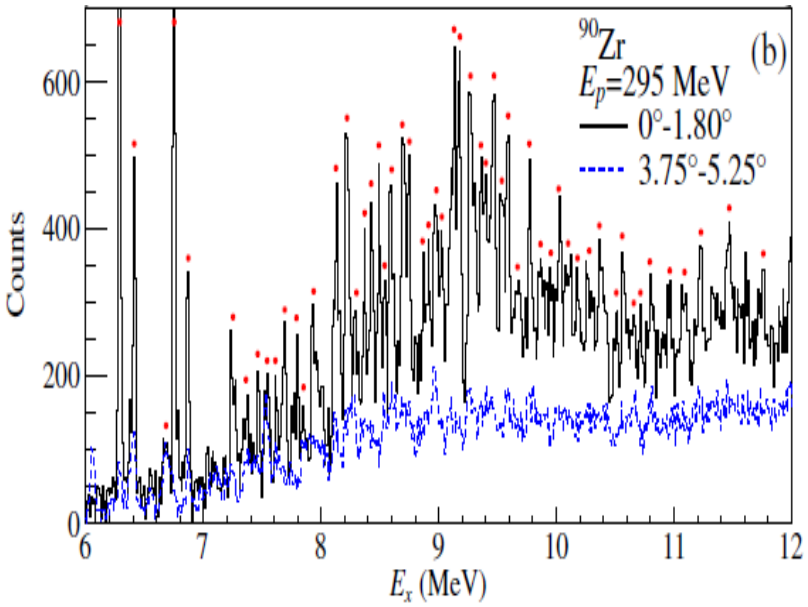

First Systematic Studies of the PDR in N=50 Isotones

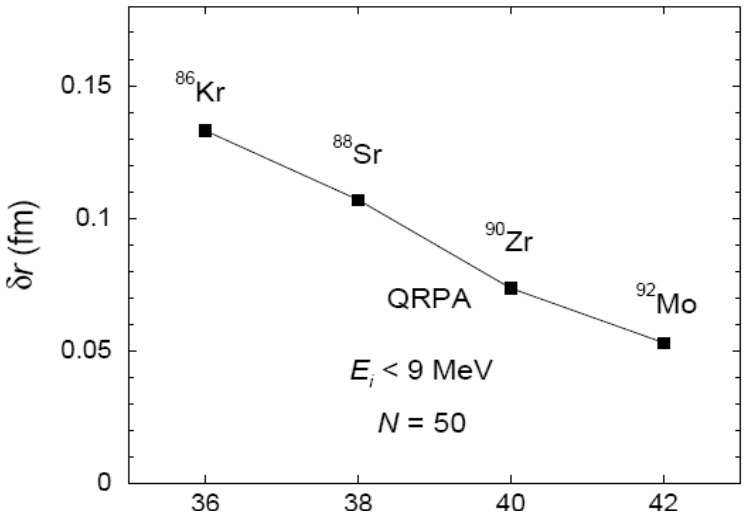

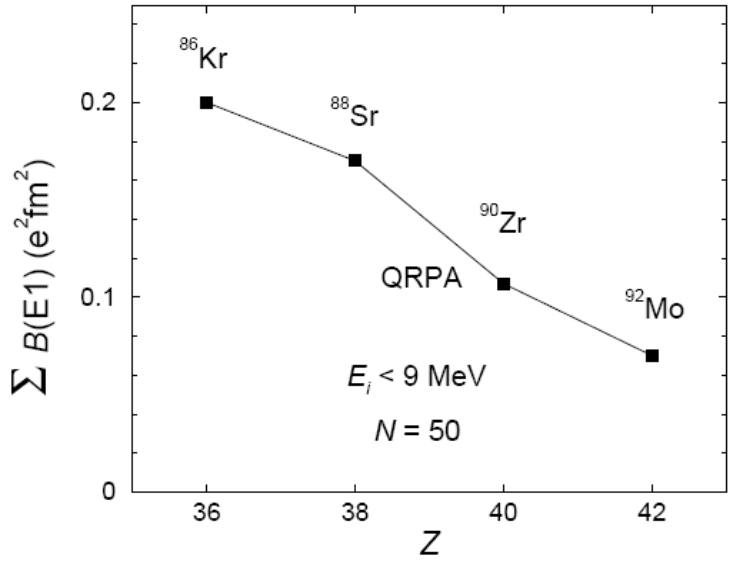

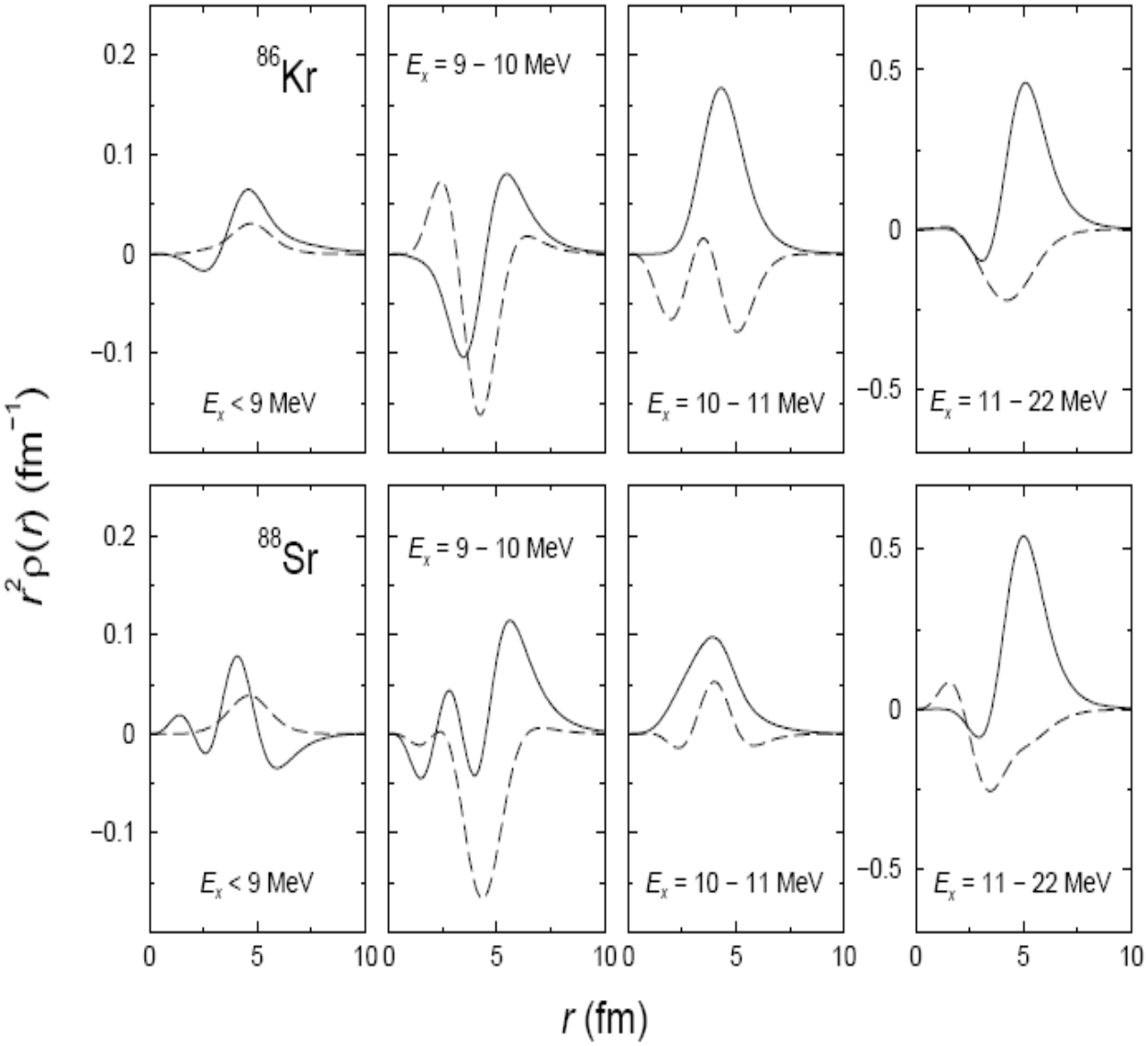

R. Schwengner et al, Phys. Rev. C 87, 024306 (2013)

Cross-Section measurements of the ^{86}Kr(γ,n) Reaction to Probe the S-Process Branching at ^{85}Kr

R. Schwengner et al., Phys. Rev. C 87, 024306 (2013);
R. Raut et al., Phys. Rev. Lett. **111**, 112501 (2013).

A way to investigate **^{85}Kr branching point and the s-process:**
^{85}Kr ground state is a branching point and thus a bridge for the production of ^{86}Kr at elevated neutron densities.

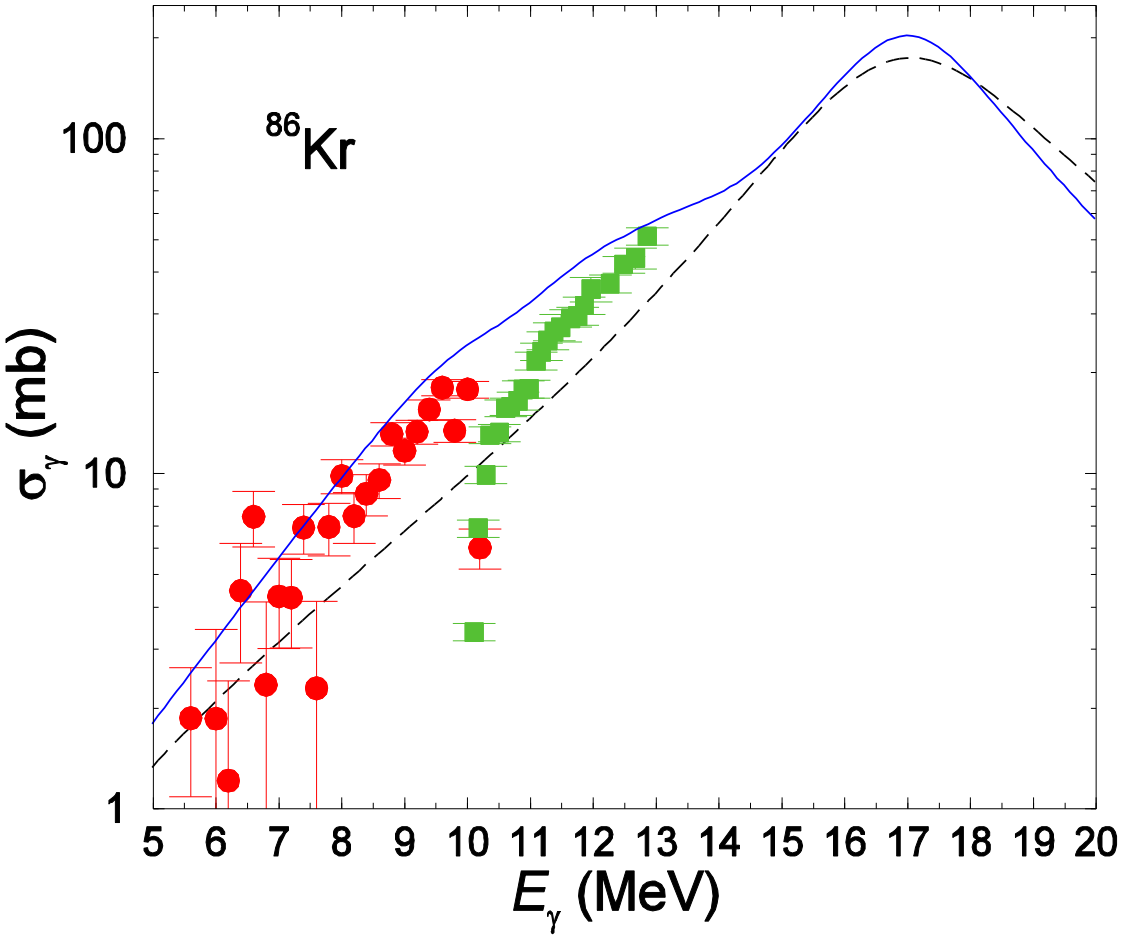

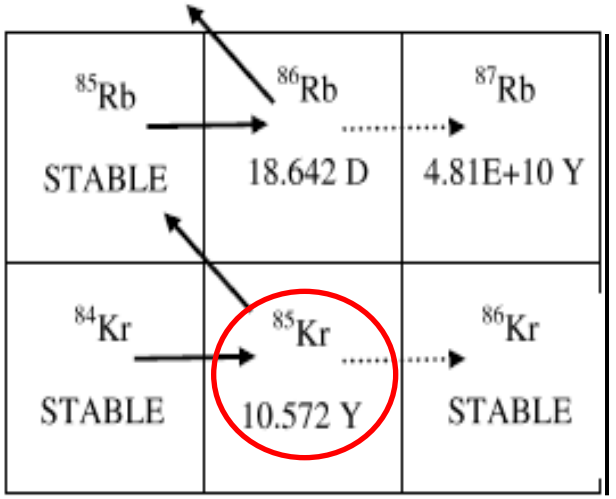

Part of the nuclear chart illustrating the *s*-process branching point at ^{85}Kr and ^{86}Rb. The solid arrows represent the usual *s*-process path while the dotted ones are the alternate *s*-process paths from branching.

Total photoabsorption cross section of ^{86}Kr

obtained **from (γ,γ') (red circles) and QRPA , 2- and 3-phonon QPM calculations.**

The QRPA and QPM solutions were folded with Lorentz curves of 0.5 MeV width.

R. Schwengner et al., Phys. Rev. C 87, 024306 (2013);
R. Raut et al., Phys. Rev. Lett. **111**, 112501 (2013).

•The QPM calculations show enhanced low-energy dipole strength in the energy region from 6-10 MeV.
•The structure of the 1^- states at about 6-9 MeV includes neutron components related to neutron skin and PDR.
•The present analysis shows that standard strength functions commonly used for the calculation of cross sections in statistical reaction models do not describe the dipole-strength distribution below the (γ,n) threshold correctly.

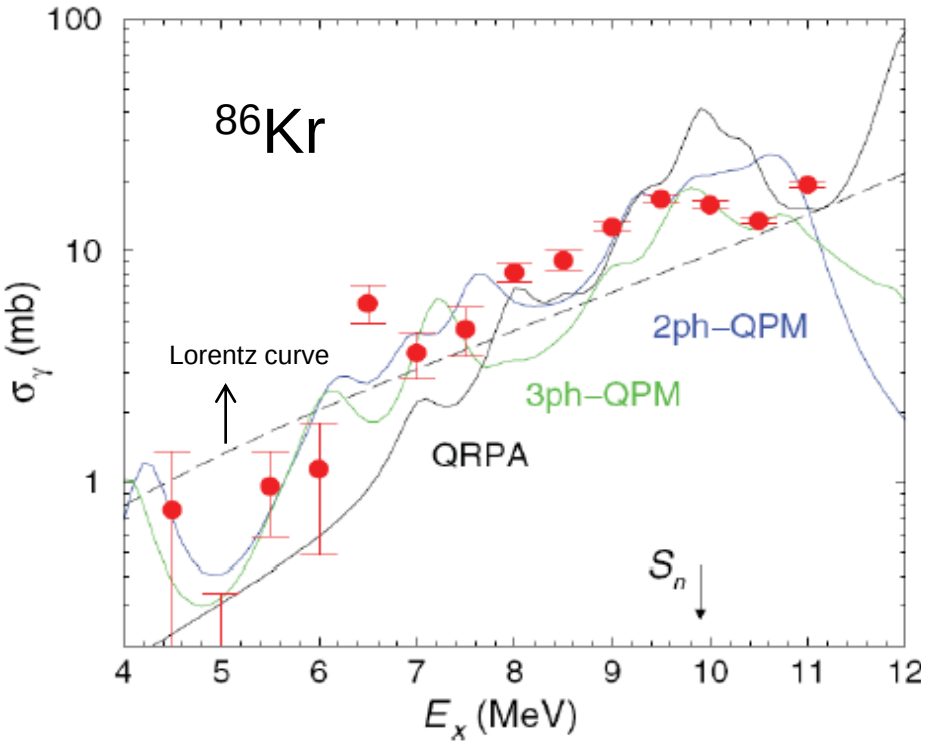

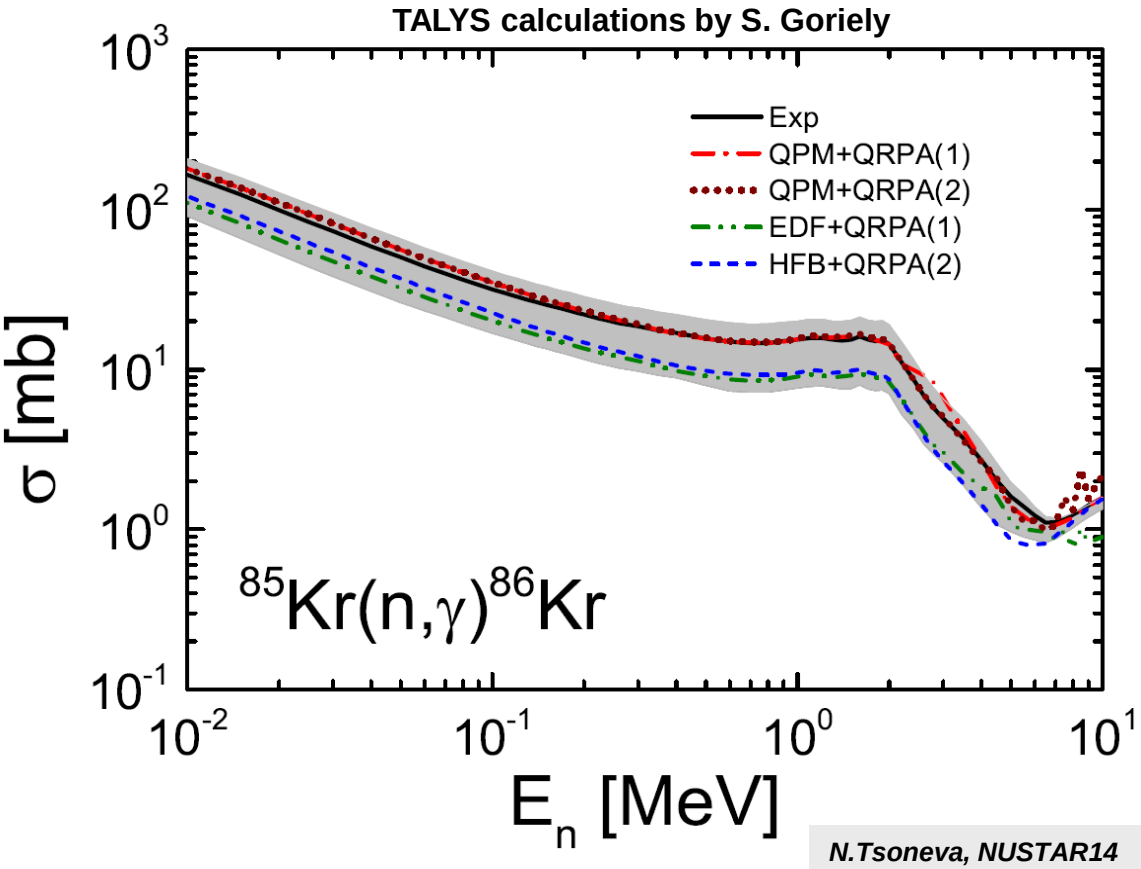

Population of ^{86}Kr in n-capture reactions related to s- and r-processes of the nucleosynthesis

s-process

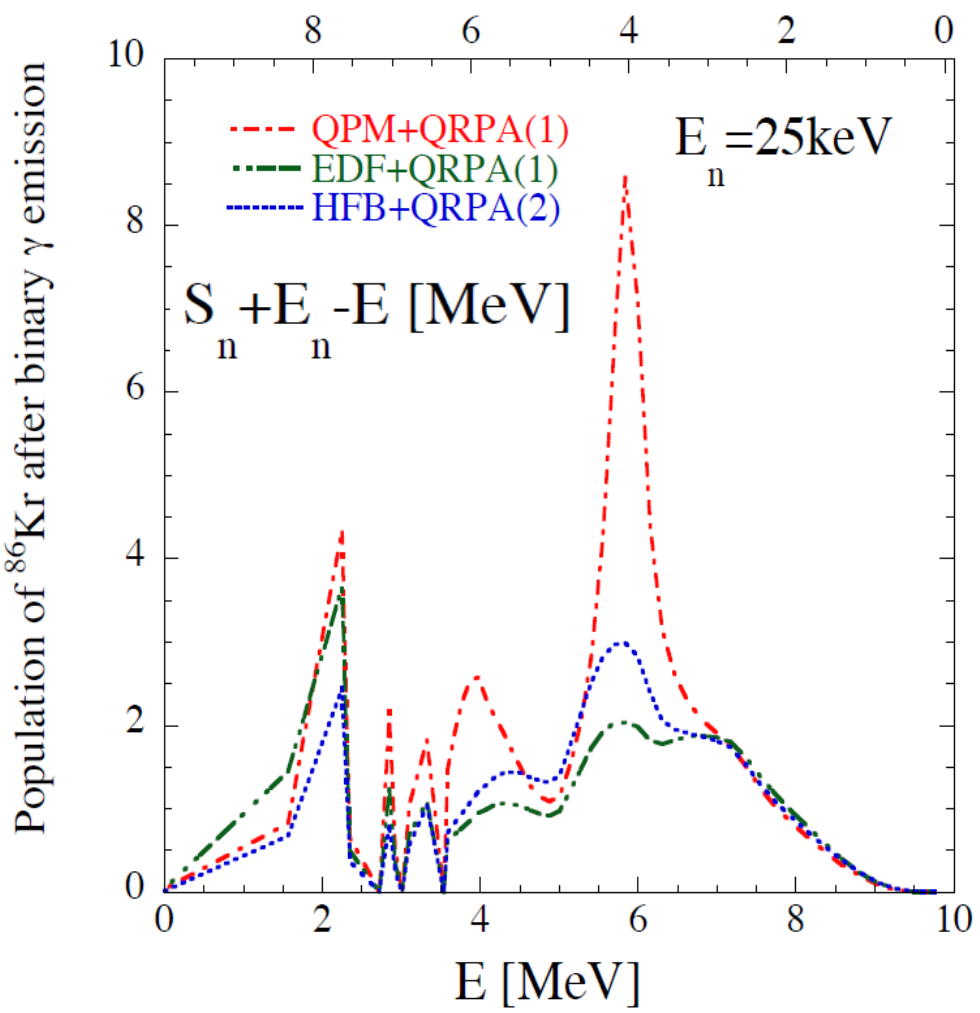

r-process

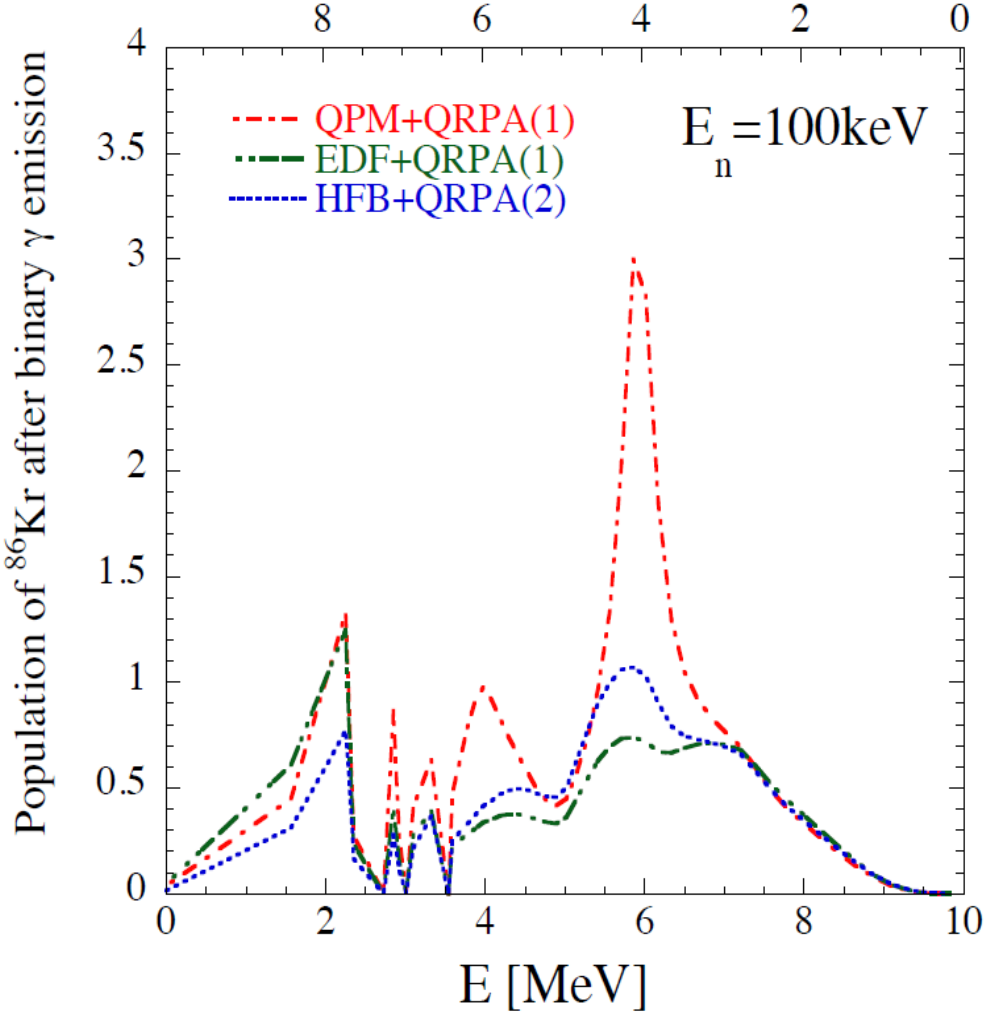

TALYS calculations by S. Goriely

Conclusions

- Systematic studies of low energy dipole excitations in N=50 reveal a concentration of PDR strength in the energy range 6-9 MeV which is correlated with the size of the neutron skin.

- QRPA is not sufficient to understand the experimentally observed fine structure of the low-energy dipole strength below and close to the neutron threshold.

- Multiphonon approach based on EDF theory and QPM describes successfully the fragmentation process of 2QP doorway states as it is seen from the comparison with experimental data on E1 and M1 strengths.

- The fine structure of the M1 resonance could be explained as a composition of spin-flip and orbital excitations related to core polarization.

- Explaining the 'quenching' of the observed M1 strength means to understand the coupling of the 2QP doorway states to many-QP configurations. The theory predicts the existence of M1 strength at and above the neutron threshold which shifts the center-of-mass of the M1 spin-flip resonance to higher energies.

- Theoretical prediction of higher order multipole excitations related to neutron or proton skin oscillations - Pygmy Quadrupole Resonance.

- The microscopically calculated strength functions could be successfully implemented in statistical reaction codes to investigate neutron-capture cross sections of astrophysical importance. The agreement with data is confirming the predictive power of involved many-body theoretical method like the QPM for exploratory investigations of n-capture reaction rates in hitherto experimentally inaccessible mass regions.